ISS Fiber Optic Failure Investigation

Root Cause Report

August 1, 2000

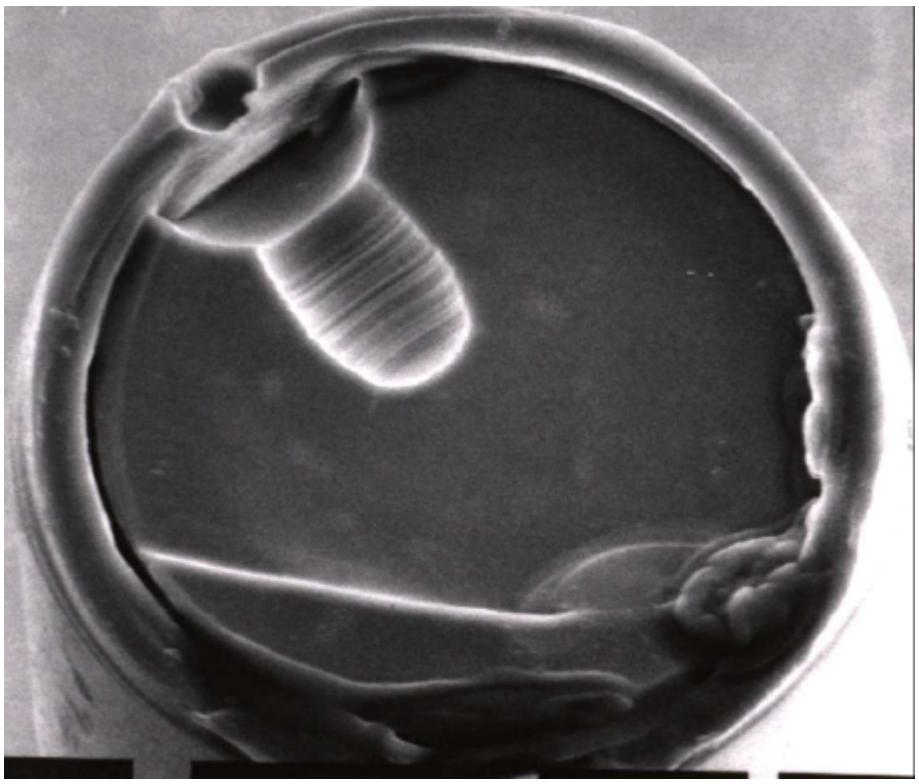

ISS Fiber Root Cause Investigation Team
Lead organization NASA GSFC
Sponsored by: NASA JSC and the Boeing Company

Table of Contents

Executive Summary……1

1.0 Introduction…….……1

2.0 Background…….……1

3.0 Cable History …….…….…….3
3.1 The Specification…….…….…….3
3.2 The Cable Design and The Performance Requirements Used……..…… 4
3.3. Indicted Stock……..…..…….7

4.0 Manufacturing Processes……..……...9
4.1 Distributor…….…….9
4.2 Cabler…….9
4.2.1 Record Keeping……..……...9
4.2.2 Storage and Factory Environment Control……..……..9
4.2.3 Respooler…….10
4.2.4 Extruder – Buffer and Jacket Processing…….……10
4.2.5 Strength Members……..……..11
4.2.6 Optical Measurements……..……11

4.3 Fiber……..11
4.3.1 Raw Materials for Preform Manufacture…….……11
4.3.2 Preform Fabrication…….…….12
4.3.3 Fiber Manufacture…….……13

5.0 Inspection Techniques and Failure Analyses……..15
5.1 Optical Detection of the Defect……..…….…15
5.2 DPA Results…….16

6.0 Material Behaviors and Interactions…….24
6.1 FEP Decomposition.…….……....24
6.2 Polyimide Related Issues…….…….……25
6.3 HF Etching……..……..……27
6.4 Carbon Layer……30
6.5 Electro Static Discharge (ESD)……31
6.6 Aeolian Motion – Vibration of Fiber Under Tension……...33

7.0 Strength Testing …….…..35
7.1 Initial Testing of ’96 Vintage Cable and ’99 Vintage Fiber.……35
7.1.1 Test Approach…….35
7.2 Strength Testing of Fiber Throughout Cabling…….38
7.2.1 Results: Strength Testing of Fiber Throughout Cabling……39

7.3 Strength Testing Non-Carbon Coated Fiber……..…46
7.3.1 Results: Strength Testing Non-Carbon Coated Fiber……...……..47
7.4 Mandrel Test Screening of Cabled Fiber…….……..50

8.0 Conclusions …….…….53

9.0 Recommendations…….54
9.1 Processes Which Create Defects…..……..55
9.2 Screening Methods…...……..55
9.3 Reducing Risks Associated with NFOC-2FFF-1GRP-1 Cable.…….…..56

10.0 References..……..56
11.0 Acknowledgements…….57

"In this work, when it shall be found that much is omitted, let it not be forgotten, that much likewise is performed…"

Samual Johnson, A.M.
For the last paragraph of Preface to his two-volume *Dictionary of the English Language*, Vol. 1, page 5, 1755, London, Printed by Strahan.

Tables

Table 1 NFOC-2FFF-1GRP-1 Optical & Mechanical Characteristics……...5
Table 2 Deliveries of PFA Jacketed Cable…….……..…..5
Table 3 NFOC-2FFF-1GRP-1 Cable Delivered by SEA Wire and Cable…….7
Table 4 Shipments Containing Reels of Cable Found with Rocket Engine Defects……..8
Table 5 Electrostatic Field Measurements Taken Around "Color Line" ……..…10
Table 6 Electrostatic Field Measurements Taken Around the Extrusion Line During a Buffering Operation…….……11
Table 7 Coating Issues & Findings……...14
Table 8 Strength Testing Samples and Conditions……..35
Table 9 Second Strength Test Approach…….38
Table 10 HF Etch Results……..44
Table 11 Strength Testing Non-Carbon Coated Fiber……...46

Figures

Figure 1 "Rocket Engine" Defect……..2
Figure 2 NFOC-2FFF-1GRP-1 Cable Design……..4
Figure 3 Crossection of the NFOC-2FF-1GRP-1 Cable……..5
Figure 4 Preform Index Profile……..12
Figure 5 Sink in the Polyimide Coating…….16
Figure 6 SiO2 Balls in PolyimideVoid..……16
Figure 7 GeO2 Crystals in Etch Pit……17
Figure 8 GeO2 and SiO2 Debris on Outside of Coating……17
Figure 9 Si-spire in Deep Etch Pit..…….……18
Figure 10 Characteristic Void in Polyimide Above Shallow Etch Pit……18
Figure 11 Defect Inspection Using Index Matching Oil…….19
Figure 12 Depressions and Bubble in Polyimide Coating in Fiber CD0588XD…….20
Figure 13 Hourglass Shape on Bubble and Polyimide……20
Figure 14 Distribution of Features Along a 6" Sample of CD0588XD Fiber…….21
Figure 15 Carbon Defects Seen Below Polyimide on Sample of CD0588XD Fiber..…21
Figure 16 E. Banks' Sample With a Broken Fiber Whose Ends Overlap...……22
Figure 17 Debris-Laden Fiber…….22
Figure 18 Cleaned Fiber..……22
Figure 19 Feature Statistics for CD0588XD..…….23
Figure 20 Feature Statistic for CD0384XC…….……23
Figure 21 Set-up for Mass Spectrometer Measurements of Fluorine Species Released From Fiber Optic Cable…..……25
Figure 22 Burn Mark Form DWV Testing of "Rocket Engine Defect" – Free Fiber……26
Figure 23 Burn Mark Form DWV Testing of "Rocket Engine Defect"……..27
Figure 24 Model of "Rocket Engine" Defect……..28
Figure 25 Stress Predicted by Fiber Model…….29
Figure 26 Etch Pit Resulting From Experimentation……..30
Figure 27 Experimentally Produced ESD Damage…….32
Figure 28 Electrical Discharge Induced Damage on Fiber Surface……32

Figures (Cont'd)

Figure 29 Test Set-up ……..36
Figure 30 Weibull Plot for Strength of 1996 Vintage Cable from Several Cable Reels ……37
Figure 31 Strength Data for 1996 Cable by Strain Rate……..37
Figure 32 Strengths of DC0384 and DC0588 Fiber During Cabling…….42
Figure 33 Example of Low Strength Breaks ……43
Figure 34 Optical Throughput During HF Etch Test ……45
Figure 35 Strength for the Non-carbon Coated Fibers ……..49
Figure 36 Mandrel arrangements and Sizes Used……..50
Figure 37 Hypothetical Break Strengths During Screen Compared to Actual Break Strengths on Proof Test Screened Sample……..51
Figure 38 Mandrel Used for Screening Evaluation……51
Figure 39 Dynamic Strength Data for the Pre-Proof Test Screened Cables……..52

Executive Summary

In August of 1999, Boeing Corporation (Boeing) engineers began investigating failures of optical fiber being used on International Space Station flight hardware. Catastrophic failures of the fiber were linked to a defect in the glass fiber (see Figure 1, "Rocket Engine Defect"). Following several meetings of Boeing and NASA engineers and managers, Boeing created and led an investigation team, which examined the reliability of the cable installed in the U.S. Lab. NASA Goddard Space Flight Center's Components Technologies and Radiation Effects Branch (GSFC) led a team investigating the root cause of the failures. Information was gathered from: regular telecons and other communications with the investigation team, investigative trips to the cable distributor's plant, the cable manufacturing plant and the fiber manufacturing plant (including a review of build records), destructive and non-destructive testing, and expertise supplied by scientists from Dupont, and Lucent-Bell Laboratories. Several theories were established early on which were not able to completely address the destructive physical analysis and experiential evidence. Lucent suggested hydrofluoric acid (HF) etching of the glass and successfully duplicated the "rocket engine" defect. Strength testing coupled with examination of the low strength break sites linked features in the polyimide coating with latent defect sites. The information provided below explains what was learned about the susceptibility of the pre-cabled fiber to failure when cabled as it was for Space Station and the nature of the latent defects.

1.0 INTRODUCTION

This report presents the work done to understand the "rocket engine" defects found in optical cable being used by the International Space Station and to understand their impact on the cable's reliability for use in space. Detailed information is given about:

- The failure of optical cable used for the International Space Station
- Techniques which can be used to inspect for the presence of "rocket engine" defects and coding defects
- The ability of the manufacturers of the fiber and cable to supply cable within the specification limits
- The suitability of the governing specification for this cable.
- Important manufacturing processes and material interactions which support HF generation from fluoropolymer cable components
- The affect of the manufacturing processes used to make NFOC-2FFF-1GRP-1 on its reliability
- The nature of the low break strength found for this cable

The members of Team 2, who generated this report and other contributors, are listed in Section 12.0. Conclusions and recommendations are summarized at the end of the report.

2.0 BACKGROUND

In mid-1999 Boeing engineers were finding multiple failures of 1999 vintage NFOC-2FFF-1GRP-1 optical cable being used to fabricate harnesses for the International Space Station (ISS) program. This cable was used in U.S. Laboratory module, an element of the International Space Station, a deliverable under contract NAS15 10000. Not only were fiber breaks being detected during handling, but breaks were found over time with no handling (sitting on the shelf). This was believed to be a much different experience than was encountered during population of the U.S. Lab module with 6982 feet [ref-1] of 1996 vintage cable of the same part number. The Boeing materials and processes engineers performed destructive physical analysis (DPA) on the fiber at the break locations. Figure 1 shows one of the first images resulting from the DPA. The cone and bulb shape of the defect earned it the name "rocket engine". This description replaced the term "bubble" which according to the fiber manufacturer, is associated with a topology that is unique and not represented by Figure 1.

Efforts were immediately made by Boeing and NASA Goddard Space Flight Center (GSFC) personnel to investigate optical inspection methods being used, to uniquely identify the stock of cable involved, and to expand the number and types of DPA images of the defect and the surrounding fiber and cable elements.

A summit was called by Boeing in October 1999 and included engineers and scientists from: various Boeing organizations (KSC, Huntington Beach, JSC), the NASA ISS parts control board, the NASA GSFC Component Technologies and Radiation Effects Branch, the cable manufacturer (BICCGeneral, formerly Brand Rex), the fiber manufacturer (Spectran Specialty Optics, now Lucent Specialty Fiber Technologies), and The Aerospace Corporation. During the summit the following overview was presented: the failure found, methods used to detect the failures, the manufacturing processes and fault trees produced by Boeing. Theories about the root cause were discussed and a plan was drafted, to initiate a formal root cause investigation, to determine the reliability of the cable installed in the U.S. Lab and to determine whether more of the same cable should be made for space flight use. Boeing retained the leadership for the latter portion of the investigation and assigned NASA GSFC the lead of the root cause investigation. This was done with NASA GSFC's concurrence and NASA JSC's concurrence and funding support. The attendees of the summit became the core of the combined investigation team.

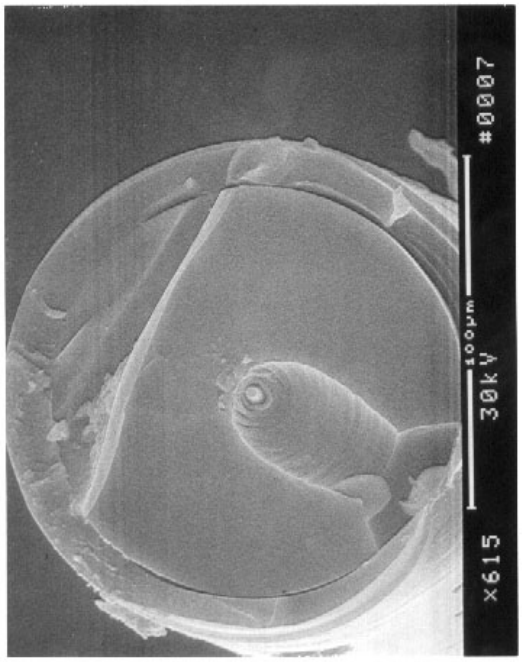

Courtesy of The Boeing Company

Figure 1 "Rocket Engine" Defect

The investigation plan included a review of the processes used by the cable distributor (Sea Wire and Cable), the cabler and the fiber manufacturer. A review of process data was performed to identify significant changes that may have contributed to the root cause. Research and experiments were also performed in support of the root cause investigation by several of the participating organizations. A preliminary review of the current cable specification was done. Strength testing was performed by Boeing in support of the cable reliability investigation. Weekly telecons were held to review the emerging information and to formulate upcoming activities. Experts from Dupont and Lucent-Bell Laboratories were invited to participate to assist in analysis of the test results being collected and to guide emerging hypotheses. Lucent-Bell Laboratories also conducted testing for the investigation.

A web site was established for the team. All photographs and documents being distributed throughout the team were posted there. A password protection system was put in place to limit access to only team members and to protect manufacturer's proprietary information.

The presentation of the hypothesis by Lucent-Bell Laboratories, which proposed that the root cause of the defect was hydrofluoric acid (HF) etching and their subsequent duplication of the defect using HF, was a turning point in the investigation. Subsequent activities focused on understanding the circumstances, both chemically and environmentally, which would support etching of the glass in this way. By understanding the conditions, which would support HF etching of the glass fiber, the failure causing defects could be identified. The team also started to consider the manufacturability of cable without these defects and/or methods, which could be used to screen them out.

In parallel with the research on the HF etching mechanism, Boeing wrote a test plan and constructed the test equipment to conduct strength testing of fiber from lots of the same manufacturing period associated with the installed cable. The intention was to make a life expectancy prediction using a statistical parameter, which determines the life of glass which ages due to stress corrosion. The lifetime prediction would also consider the stress and temperature conditions the installed fiber will experience due to how it was installed within the cable and within the spacecraft structure, the stresses associated with launch, and the presence of a moist ambient environment in space. Testing was performed on fiber that was still contained in the cable (finished product) and though the data did not clearly provide a quantifiable reliability number, it did show that even after the "rocket engine" defects were screened out, the fiber had low break strength. End faces of the cabled fibers, which broke at low strength, were inspected and they all featured a characteristic bubble-like feature in the polyimide coating and bare glass surfaces, which have been etched or corroded. This evidence is believed to indicate that discontinuities in the fiber coating are allowing both the "rocket engine" etch pit and low strength associated with moisture enhanced stress corrosion.

A second summit was held by Boeing in February 2000 to summarize the progress made by the team, to formulate a plan for future use of the installed cable and to plan for the purchase of new cable. New teams were established for the following action areas: 1) cable redesign, specification rewrite and cable qualification, 2) Root cause wrap-up, 3) Maintenance plan for on-orbit repair inside the module, 4) Maintenance plan for extra-vehicular on-orbit repair, and 5) Plan for a shuttle mission experiment to understand in-flight risks associated with this cable. This report is the final deliverable for Team 2.

3.0 CABLE HISTORY

3.1 The Specification

The optical cable being used by Boeing on ISS is governed by the NASA specification SSQ 21654, "Cable, Single Fiber, Multimode, Space Quality, General Specification for". The custodian of the specification is McDonnell Douglas Space Systems Company in Huntington Beach, CA. This organization is now owned and operated by Boeing. The most recent approved version is Revision B, dated June 28, 1996 [ref-2]. A change revision was made by Boeing, named SSCN 000904, which affected most of the paragraphs. This change notice is not dated. A draft of revision C also exists, but was never approved for use.

A cursory review of Revision B by GSFC identified significant problems with the specification and indicated that it does not accurately describe the physical characteristics and performance of the cable that is being used and does not adequately define the qualification requirements. The condition of the specification is not considered to be a leading cause of the failure of the cable. Team 1, described in the Background section above, may produce a new version, which will supercede all of these previous versions.

3.2 The Cable Design and The Performance Requirements Used

Two part numbers were defined in Revision B and the change notices: NFOC-2TFF-1GRP-1 and NFOC-2FFF-1GRP-1. The former was for a PFA jacketed and PFA buffered design and the latter was for a FEP jacketed and FEP buffered design. Table A-1 of SSQ 21654, Revision B., SSCN 000904 summarizes the optical performance ratings and cable component materials and dimensions, and is included here as Figure 2 and Table 1 below. The corresponding part number to Figure 2 and Table 1 is NFOC-2FFF-1GRP-1. A crossection is shown in Figure 3.

Find	Item	Dimension	Material	Construction
A B	Core Cladding	100 ± 2µm 140 ± 2µm	Doped Silica	Drawn
C	Hermetic Coating	0.025-0.05 µm Thickness	Carbon Based Hermetic Sealer	Chemical Vapor Deposition
D	Fiber Coating Buffer	170 ±2 µm	Polyimide	Coat with Heat Cure
E	Cable Buffer	380-760 ± 25µm	FEP-Teflon	Extruded
F	Strength Member	1.6mm OD	Teflon Impregnated Fiberglass	Braided
G	Cable Jacket	2.10 ± 0.05mm .25mm Thick	FEP-Teflon	Extruded

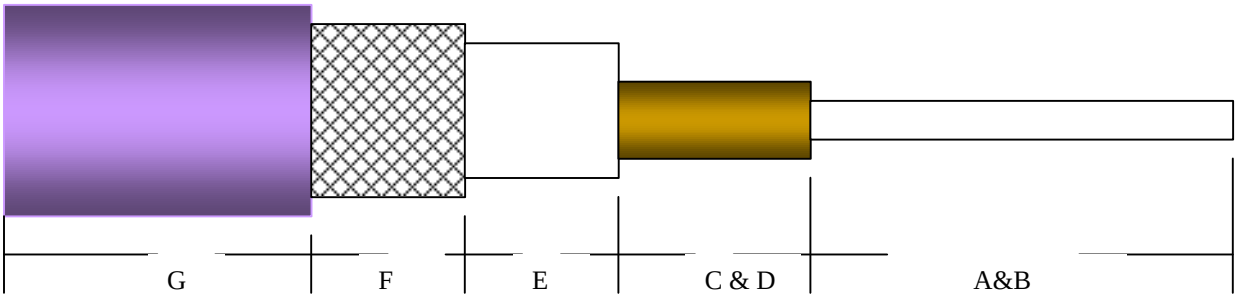

Figure 2 NFOC-2FFF-1GRP-1 Cable Design

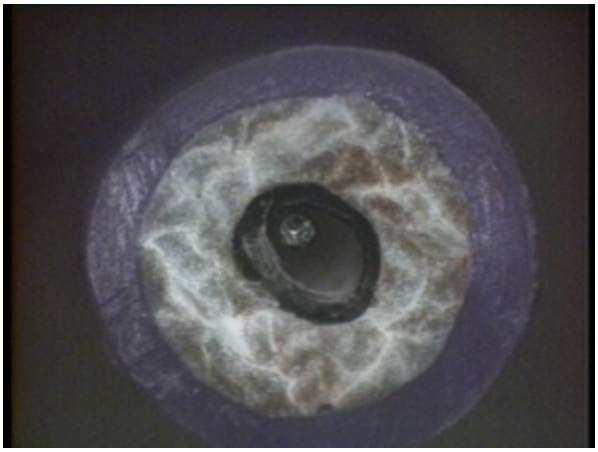

Courtesy of NASA GSFC

Figure 3 Crossection of the NFOC-2FF-1GRP-1 Cable

Table 1 NFOC-2FFF-1GRP-1 Optical & Mechanical Characteristics

Characteristic	**From SSQ 21654, SSCN 00904**
Attenuation	4 dB/km @ 1290 ± 10 nm
Numerical Aperture	0.30 ± 0.02 @ 1290 ± 10 nm
Bandwidth	200 MHz-km @ 1290 ± 10 nm
Proof Strength	200 kpsi minimum
Core Ovality	5%
Cladding Ovality	4%
Core/Cladding Offset	98% minimum
Cable Weight	5.5 lbs/1000 ft. maximum
Color	Violet per Mil-Std-104
Temperature	Operating: -100°C/+75°C Storage: -100°C/+85°C

Order sheets were reviewed by Boeing and an inspection of the U.S. Lab was done by Boeing to understand how much of the NFOC-2TFF-1GRP-1 (PFA/PFA) cable may have been used in the U.S. Lab. SEA Wire and Cable (SEA) provided information about orders delivered for both the NFOC-2TFF-1GRP-1 and NFOC-2FFF-1GRP-1 cable. Table 2 shows the lengths of NFOC-2TFF-1GRP-1 cable ordered by several users.

Table 2 Deliveries of PFA Jacketed Cable

Invoice Period	**No. of Orders**	**Customer Name**	**Total length ordered (ft)**
8/11/93	1	MTP Aircraft	525
3/6/95 & 8/14/95	2	Boeing Huntsville	45
9/6/95	1	Spar Aerospace (CAE Electronics)	700
9/18/95	1	McDAC (Boeing HB)	5000
12/95	1	ITT Cannon	4500
3/30/95	1	Space Systems Loral (for Japan)	197
4/20/95	1	Standard Wire and Cable	434

The equipment inspection did not find any NFOC-2TFF-1GRP-1 (PFA/PFA) cable in the U.S. Lab. Evidence is not definite about the use of –2TFF- in ISS element Node 1. A list of Node 1 harnesses, prepared as part of another effort, indicates 1 harness containing 10 links is constructed of -2TFF-. The total length of –2TFF cable, per this list, is approximately 200 feet [ref-3]. The material delivered to ITT Cannon is believed to have been used in the development and qualification of the connectors used by ISS. NFOC-2TFF-1GRP-1 is no longer being used because its optical loss was found to increase after thermal cycling due to excessive shrinking of the PFA material (jacket and buffer shrinkage was not controlled by the specification requirements).

Table 3 in Section 3.3 shows the NFOC-2FFF-1GRP-1 cable delivered by the sole distributor, SEA Wire and Cable to various customers. BICC's shipping certificate of compliance references the cabler's internal part number, OC-1614, and contains a sentence at the bottom indicating that the cable was "manufactured to and acceptance tested in accordance with the SSQ 21654, and CR SSQ 21654-008".

SEA performed cable outer diameter (OD) measurements at each end of the reel as an acceptance measurement. For all other acceptance measurements, SEA used BICCGeneral generated "Certified Test

Data" to document the conformance of the cable to the specification requirements. Samples of these documents were provided by SEA and BICCGeneral. Ten of the 25 design characteristics reported by BICCGeneral are recorded on a go/no go basis; ten are referenced to a "Spectran" inspection, and five are shown as a measured characteristic. *["Spectran" refers to the fiber manufacturer, formally known as Spectran Specialty Optics Company and now called Lucent Specialty Fiber Technologies or Lucent-SFT]*. Several other identifying numbers are shown on the sheet including reel number, date, customer order number, BICCGeneral part number, Date of Manufacture (DOM) and length. The BICCGeneral part number used was OC-1614. A footnote at the bottom of the sheet indicates that the material is made and tested in accordance with SSQ 21654.

All of the requirements referenced on the test data sheet correspond to those listed in Figure 2 above. During a review of the processes used at BICCGeneral, the attenuation and cable layer dimensions measurements done by BICCGeneral were found to be in accordance with the specification requirements.

BICCGeneral ordered the fiber from Lucent-SFT in accordance with a build specification numbered BF04515. A review of the processes used at Lucent-SFT showed that they were performing optical and visual inspections correctly including fiber geometry measurements.

Issues were identified with respect to the manner in which the proof test is executed at Lucent-SFT. An industry standard proof test is defined by EIA-FOTP-455-31, Fiber Tensile Proof Test. This test method specifies that the user specified minimum tensile stress is maintained on the fiber for a minimum time of 1 second. Lucent-SFT's implementation of the proof test in-line with the fiber draw process does not achieve this dwell time. It was recommended that Lucent-SFT also add a bend in a fourth axis to achieve a test that exposed more of the fiber surface to the tensile load. Strength testing done by Boeing on virgin BF04515 fiber (never put through any of the cabling processes) showed results above 5 lbs.

The cable specification requires the fiber used to meet a minimum proof strength of 200 kpsi, (which corresponds to 5 lbs of tension for this fiber), though it does not detail how that strength should be established. Since in-line proof testing is fairly common throughout the industry, the EIA test method needs to be revisited to provide a high-speed test or to disallow it. The SSQ documentation will have to do the same.

Both the fiber manufacturer, Lucent-SFT, and the cabler, BICCGeneral, were found to be delivering product in accordance with the details shown in Figure 2 and Table 1 above with the exception that the fiber proof test was not achieving a 200 kpsi load on the fiber.

3.3 Indicted Stock

A review of all NFOC-2FFF-1GRP-1 cable delivered by SEA and BICCGeneral to Boeing-Huntington Beach (Boeing-HB) and Boeing-Kennedy Space Center (Boeing-KSC) was performed by examining the shipping records. Several spreadsheets were developed by each organization to summarize the findings. SEA provided information about lengths ordered, by whom and the date of manufacture (DOM) for the cable (and its shipment date). BICCGeneral supplied records including cable reel numbers, order numbers, DOM and some traceability to fiber lot. A great degree of inconsistency exists regarding the use of the term "lot" and as a result, several significant blocks of traceability data do not exist. Table 3 shows the amount of NFOC-2FFF-1GRP-1cable delivered by SEA.

Table 3 NFOC-2FFF-1GRP-1 Cable Delivered by SEA Wire and Cable

Invoice Period	No. of Orders	Customer Name	Total Length Ordered (ft)	No. of Reels*
6/12/96 & 7/26/96	2	MCDAC Huntsville	5031	8
6/26/96 to 12/30/98	14	ITT Cannon	7423	
7/17/96 to 4/1/99	14	Boeing Huntsville	40,695	41
7/19/96	2	CAE Electronics	500	
7/24/96 to 5/7/99	27	Boeing Huntington Beach	109,346	
7/25/96 to 11/25/98	10	Nakano Aviation	9453	
8/9/96	1	Amphenol	1200	
9/5/96 & 5/1/97	2	Space Systems Loral	8990	
11/15/96 & 2/17/97	2	Pacer	600	
3/26/97	1	NTK Aviation	1000	
5/28/97 & 4/7/99	2	Electronic Conn	701	
6/17/97	1	Standard Wire and Cable	100	
7/18/97 to 11/25/98	7	OHB Systems	11,596	
10/6/97	2	Boeing Downey	1496	4
1/23/98	1	TRW Components	168	
7/13/98	1	Boeing Seattle	100	
11/30/98 & 5/7/99	2	Lockheed-Martin Houston	600	
11/30/98 to 8/17/99	5	Boeing KSC	9575	8
12/16/98 & 7/2/99	2	Prime Cable	800	
1/20/99	1	Elymat Industries	89	
6/25/99 & 7/12/99	2	Undefined	400	

*No entry indicates number of reels was not researched.

Preliminary findings and discussions identified several significant periods in the production and use of the cable that were thought to be unique with respect to the number of defects found and the process changes made. The abruptness with which these types of defects surfaced seemed to indicate that some part of a once stable, validated, process had gone out of control. All of the cable delivered to Boeing and not already installed in the U.S. Lab was screened optically, with visual fault finders. Glows and echos were found in reels manufactured in 1998 and 1999. No 1996 era product was available for test until several reels in bonded storage at SEA, were returned to Boeing (these had been returned to SEA by Boeing for "out of specification" roundness). One glow, which was found to be a "rocket engine" defect, was found in one of these 1996, out-of-spec reels. No 1997 era cable was found for test.

Table 4 Shipments Containing Reels of Cable Found with Rocket Engine Defects

BICCGeneral SHIP DATE (always within 1 wk of manufacture date)	Cable Length Dlvrd to SEA (ft)	Number of Reels Screened*	Number of Reels Found with Defect(s)
12/22/95	545		
2/16/96	200		
6/12/96	1900		
6/17/96	1718		
6/18/96	640		
6/25/96	2555		
8/1/96	2655	5	0
8/29/96	6836		
9/26/96	22060		
12/19/96	7048	6	1
11/21/97	15574		
2/28/98	384		
7/21/98	4998	5	2
8/25/98	698		
8/27/98	9594		
8/28/98	3402	4	0
11/24/98	20044	1	1
3/31/99	15710	14	13
4/1/99	7092	9	7
4/30/99	20286	12	3

*No entry indicated and no screening performed on associated lot.

No uncabled fiber of 1996 vintage was available for examination. Five reels of 1998 BF05202 fiber, which had never been cabled, were available at GSFC through another flight project (BF05202 fiber uses the same preforms and draw processes as the BF04515 except that slightly different cladding and coating outer diameter specifications are used). No glows were found in these reels (~3,000 ft of fiber).

The links installed in the U.S. Lab were not each inspected with either a visual faultfinder or an OTDR due to the lack of equipment and manpower resources. This precludes determining the relationship between the quality of the installed cable and the quality of the samples that were available for test, but were of a different manufacturing period.

Oral histories were taken from people involved in the assembly of the harnesses used in the U.S. Lab. The technicians indicated that there was an unusually high amount of scrap but that it wasn't considered high enough to stop production for failure analyses. The failures were attributed to handling, which may have been a logical assumption for a team new to working with fiber. It may also have been the result of an inadvertent defect screen. Some breaks were found in integrated harnesses in the U.S. Lab but they were typical of failures due to overstress at connector backshells.

The "rocket engine" defect in the 1996 cable and the speculation that some "rocket engine" defects may have been discarded in the scrap associated with the U.S. Lab harness builds, caused the team to suspect that the "rocket engine" defect and the low strength failure mode was ubiquitous to the NFOC-2FFF-GRP1-1 cable.

4.0 MANUFACTURING PROCESSES

The manufacturing processes used by SEA, BICC and Lucent-SFT were discussed regularly during the investigation. Reviews at each of the respective plants (two for Lucent-SFT) were performed in order to understand the processes being used and their possible contribution to the creation of the defect.

4.1 Distributor

Boeing-HB led the review and performed a data traceability review for six NFOC-2FFF-1GRP-1 1996 era cable reels. Some records were found while others were not. SEA processing required only measuring OD, cutting cable to length (including a respooling process) and re-labeling the spools of cable received from BICC. All cable shipped to Boeing-Huntsville (Boeing-HSV) was respooled to plastic reels from wood reels. There were no processes found at SEA to be damaging the cable and causing the rocket engine defect.

4.2 Cabler

BICC generally delivered the cable to SEA within six days of its manufacture. Twenty (20) deliveries to SEA were made between 12/95 and 4/99, mainly centered around: the second half of 1996 (46 kft total), 11/21/97 (15 kft), 10/98 (39 kft), and 4/99 (43 kft). The records show no production other than these four periods.

A comparison of the shipment records to the reels identified with the "rocket engine" defects did not clearly show an abrupt increase in defective cable corresponding to large changes in either production volume or cable length. There were distinct periods of high throughput and shipment of multiple short lengths. A review of some of the corresponding purchase order information indicates that the short lengths were not specified by the buyer.

The processes given the most attention during the review at the BICC facility were the records keeping, fiber respooling, extrusion and the optical measurement processes. Later discussions focused on the extrusion process because findings were revealing that the extrusion conditions were very likely causing a generation of HF which acts as an etchant when it contacts glass.

4.2.1 Record Keeping

Records for six reels of cable were exhumed. Most of the materials traceability was not recorded. A buffer run sheet, which specifies manufacturing settings/conditions and specifications for a given product, is provided to the extruder operator to record the events of the run. These sheets were not filled out properly for the reels of interest, more so for the 1996 timeframe. The record keeping has improved over the period that the NFOC-2FFF-1GRP-1 has been made at BICC, however it is still not sufficient to show a complete traceability history. There is no fiber traceability, for example, for most of the reels made in 1996 – the vintage used to populate the US Lab module.

4.2.2 Storage and Factory Environment Control

"The environmental conditions of the extrusion facility were kept to 21 to 24 degree C and 45% to 50% relative humidity. Fiber storage was controlled in a separate area with limited access. The cable manufacturing location, containing two extrusion lines, were also outside of the general walking traffic. All processes following re-spooling and fiber storage were performed in the same room.

4.2.3 Respooler

Correspondence records supplied by BICC showed that in January of 1997 McDonnell Douglas (Now Boeing-HB) notified them that the polyimide coating on the fiber in the NFOC-2FFF-1GRP-1 cable, was dimensionally out-of-specification. This was confirmed by Boeing-HB personnel who were not able to terminate the fiber in the connector ferrules because its outer diameter (OD) was too big (following return of the product it was realized that the wrong fiber part number was cabled and shipped). Between 3/97 and 10/97 arrangements were made to use a LaserMike™ laser based measurement device installed on a fiber coating machine to screen the fiber for out-of-spec OD. This equipment, a Nokia OFC52, was normally used to add colored coatings to fiber for identification purposes, and is often referred to as a color-line. Use of this system as a screen was first used on 10/7/97 and became a permanent process for the NFOC-2FFF-1GRP-1 cable thereafter. Adjustments were made in April of 1998 to resolve calibration issues.

The respooling process was considered a possible source of ESD that could be damaging the fiber. A discussion of the susceptibility of the polyimide to breakdown and subsequent current flow in the carbon coating is presented in Section 6.1. Electrostatic field measurements were made during a respooling operation on the color-line using the BF04515 polyimide/carbon coated fiber (the ambient relative humidity was 45%). Two meters were used, a 3M 709 Static Sensor and a Plastic Systems 42720 Static Field Meter. These meters are intended for measuring fields extending from charged, flat plates. At the time of the release of this report, agreement was not reached regarding the interpretation of the measurements recorded and shown in Table 5 because the geometries that were measured were varied and not plane sources.

Table 5 Electrostatic Field Measurements Taken Around "Color Line"

Location	**Field During 20 m/min operation (V/inch)**	**Field During 50 m/min operation (V/inch)**	**Field During 20 m/min operation (V/inch)**	**Field During 50 m/min operation (V/inch)**
	3M 709 Measurements		Plastic Systems 42720 Measurements	
Let-out reel	+40	+25	-200	+640
1st pair of tension control wheels	+30	+110		
Pre-ionizier wheel	-2000	> -10,000	+350	N/A
Post-ionizer			-980	-900
Entrance into wheel/belt section	-140	-1150	-300	-3500
Exit out of wheel/belt section	-35	-65		0
Pre-OD detector				-500
Post OD detector	-25	-45		
Take-up reel	+85	+50	+50	-300

4.2.4 Extruder – Buffer and Jacket Processing

BICC demonstrated the operation of the extruder after the FEP pellets were added and melted in the reservoir. The original shipping containers were kept near the secondary containers, which showed the color of the pellets and were marked with the name of the material. The conditions for heating the pellets, the extrusion temperature, and the extrusion rate were reported by the process engineer. No special precautions were taken to avoid creating corrosive decomposition products from extruding in air such as baking out the pellets and confining the extrusion atmosphere to something other than air. Temperatures ranged between 288°C (exposure to air following extrusion) and 404°C during the extrusion process.

Immediately following extrusion, the cable passes through two water baths. The same process, with a different extrusion head, is used when applying the jacket. The extrusion line was reviewed with the field meters the results of which are shown in Table 6.

Table 6 Electrostatic Field Measurements Taken Around the Extrusion Line During a Buffering Operation

Location	**Field (V/inch)**
Let-out reel	-750
Air space between quenching baths	-150
Exit of second quenching bath	-10
Length counter (wheel & belt)	*
Rubber belts – entry	-110
Rubber belts – exit	-45
Tension wheels – 1st	+2000
Tension wheels – 2nd	+2250
Tension wheels – 3rd	+75
Ground chain	-100
Metal feeder wheel	+305
Take up reel (in path of de-ionizing fan)	-1500

* Did not capture numerical data but recollection is that it was near the minimum floor of 50V/inch.

4.2.5 Strength Members

The equipment and materials used for applying the braided strength members to the buffered fiber were briefly reviewed and found to be industry standard with no detail that seemed related to the fiber failure. BICC reported that the only time they rejected finished NFOC-2FFF-1GRP-1 cable was when lumps were found under the jacket due to the strength members (associated with the change out of a spool of the strength member material, Teflon™ impregnated fiberglass). Lengths with this defect were cut out and not delivered to SEA.

4.2.6 Optical Measurements

Both a Tektronix™ TFP2 FiberMaster and a GNNettest™ CMA 4000 are used, at 1300 nm wavelength, for measuring attenuation. The equipment and set-up were witnessed and nothing was found that would indicate incorrect measurements were being recorded or that the method being used contributed to the fiber defect. BICC reported that they had not rejected any reels of cable based on optical performance.

4.3 Optical Fiber

Great attention was also paid to the details of the fiber production processes in order to understand the root cause of the defects and if any conditions were found which could isolate them to specific lots or periods of production.

4.3.1. Raw Materials for Preform Manufacture

Lucent-SFT makes their own glass preforms. The applicable raw materials are the natural quartz cladding tubes and the gases. The gases are monitored for quality on an incoming sample basis and are monitored daily, in-line, for water content. The tank farm for most of these gases (some come in transportable cylinders) was moved between 1996 and 1997. There was no strong evidence indicating that the move of the tank farm or the handling of the gases allowed contamination of the gases or contamination of the preform manufacturing processes.

The pure fused silica substrate tubes are reviewed for defects and records are kept allowing traceability between the raw material and the finished preform. Many of the preform build records showed a great degree of "flaws" in the tubes however this is normal in natural quartz. These features in the received quartz tubes have not been connected with the "rocket engine" defects or the low break strength and have not been investigated further.

4.3.2 Preform Fabrication

The BF04515 fiber is drawn from preforms uniquely identified by a part number containing the number 320-R. All "320-R" preforms are made on one lathe, which is reflected in the preform part number. This lathe is also used to fabricate several other preforms whose recipes use all of the same ingredients as those used for the "320-R" product or a subset thereof. The "320-R" preforms are also the originating material for several other variations of fiber dissimilar to the BF04515 only in the glass and coating tolerances. The "320-R" lathe is located apart from the main production area in an area reserved for R&D activity, is air-conditioned and is humidity controlled. R&D operators are selected from the experienced pool of operators who make standard Lucent product.

The build sheets include requirements for the gas mixture, the process recipe and spaces for recording observations and process variations. Tweaking of the process recipe is allowed within engineered specified limits and is performed by the specially trained preform technicians who run the equipment and monitor the fabrication run. When a slight change is made for this purpose, it is saved as part of the current preform recipe. The recipe revision in place during each preform run is recorded on the build sheet. That recipe revision will stand until another change supercedes it. The dimensions of the finished preform and defects or features, such as bubbles and airlines, observed in the preform are also recorded. A refractive index profile is measured for each preform in a separate laboratory. An example of one is shown in Figure 4 [ref-4]. The "MESA" database is used to link the preform records with the records for the finished fiber. This automated filing system was started in the second half of 1996. A paper system predated the use of the "MESA" system.

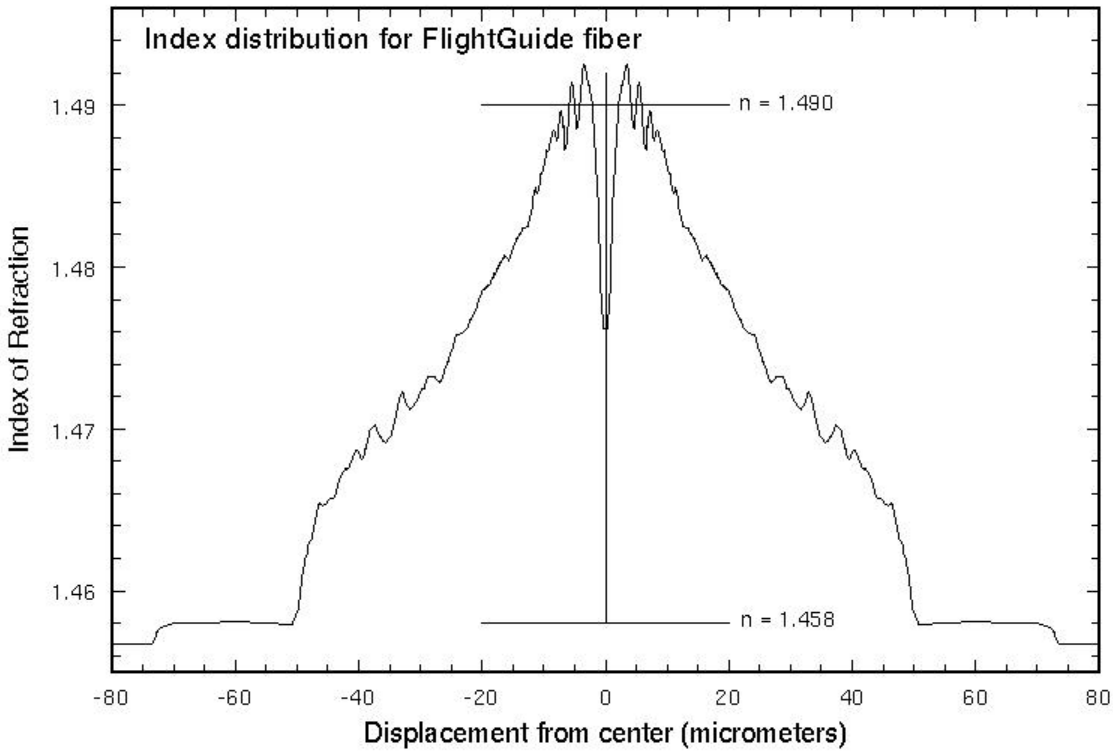

Figure 4 Preform Index Profile

Preform processing includes cleaning and etching the substrate tube and the finished preform. Both a hydrofluoric acid bath and fire polish are used. These methods along with the CVD method for growing the core/cladding transitional layer and the core, eliminate the possibility that contamination was trapped between the core and cladding, inside of the core or in the surface of the cladding layer of the preform. The creation of a void inside of the preform due to an inside contaminant could only take place during the major neck-down of the preform during the fiber draw process. This would produce a defect elongated by at least some significant fraction of the drawdown ratio, which is approximately 12,000:1 in the longitudinal direction. This amount of elongation is quite the opposite of the shape of the radially elongated, bulb shaped defect that is the subject of this report.

A review of the preform records showed manufacture of 181 "320-R" preforms between 11/94 and 8/98, the heaviest period of production of being between July of '96 and April of '97. Of these 181, 17 were traceable to NFOC-2FFF-1GRP-1 cable. Eight were associated with reels found with a "rocket engine" defect. All preforms used for the Boeing fiber were produced prior to August of '98, and were held in stock up to a year before they were drawn into fiber.

4.3.3 Fiber Manufacture

A review of the fiber draw and cabling facility in Avon, CT was performed. Though the traceability between the cable and the fiber is not complete for much of the pre-1997 cable, the records indicate that at least 81kft of fiber in the NFOC-2FFF-1GRP-1 cable was drawn at the current facility and 53kft was drawn at a facility which has since been decommissioned. The fiber drawn for the NFOC-2FFF-1GRP-1 cable is called BFO4515 by Lucent-SFT.

The current facility, at Darling Drive in Avon, CT, contains several draw towers although all of the BFO4515 fiber was drawn on a single tower that is part of the fiber reel number. The draw room is temperature controlled to around 22°C and limited to traffic through a clean-room entrance (approved personnel only, smocks required, etc.). An auxiliary glass lathe for fire polish is kept in the same area as the draw tower. In-line and end-of-line test equipment are run along side the tower controllers and computers.

The build records start by instructing the draw operator how to manually set the tower settings which include draw speed, iris settings, gas flows and cure temperatures. A two-axis laser based micrometer is used with an active control feedback to the glass furnace. The control loop allows real-time adjustment of the draw speed in order to maintain the required glass outer diameter. The reactor for the carbon coating is located immediately below the draw furnace, which is at the top of the tower. The polyimide coating is applied in several stages below the draw furnace. The polyimide forming material is delivered to the coating applicator cups. Coating die size, incoming fiber size, draw speed, and material viscosity (temperature controlled) determine the actual volume per unit length deposited onto the fiber. The coating application dies are fabricated from specialized materials in order to preserve the ultra high precision required over multiple draws.

The draw operator looks for defects in the coating as an in-line acceptance screen during draw. Coating defects are inspected visually and by "feel". A LaserMike™ -based, four-axis inspection system is in place in-line to detect coating thicknessess out of specification. This second set of laser micrometers do not have an active control loop with the coating process. They trigger an alarm when the geometry limits are not net and the draw operator must react appropriately.

All of the BF04515 fiber was proof-tested in-line during the draw/coating process using a 3-plane mandrel system. Lucent has recently increased the number of mandrels/planes to 4. The review team is not in agreement regarding the proper execution of an in-line proof test that will expose the coated fiber to a minimum 200 kpsi for a minimum length of time. Recommendations about how an in-line proof test should be done, will be submitted under separate cover to the EIA/TIA for inclusion in the standard test method.

Following the completion of the draw/coating process, the fiber is measured for its optical performance, a resistance measurement for the carbon coating is taken and coating geometry measurements are made at a test bench. Bandwidth measurements are made at three wavelengths, loss measurements are made at approximately 6 wavelengths including 1380 nm for the water peak. Numerical Aperture (NA) is measured at an unspecified wavelength. The resistance measurement is used for screening the quality of the carbon coating. Geometry measurements include: core and cladding diameter, core and cladding noncircularity, clad/core concentricity, polyimide coating diameter, and coating concentricity.

When non-conforming sections of fiber need to be removed from the reel, the fiber is respooled under a de-ionizing fan used to remove charge. Sub-spools of a single draw lot are assigned the same draw lot number and a unique letter identifier suffix for the spool.

The carbon and polyimide coating processes were reviewed during the on-site visit and were discussed several times over the period of the investigation to understand how they may contribute to or support the root cause of failure. Table 7 lists the concerns investigated and the corresponding findings.

Table 7 Coating Issues & Findings

Issue	**Finding**
Is there an opportunity for debris to fall into the coating cups from the carbon application station	An exhaust system is used below the reactor to prevent this.
The temperature of the carbon application process could be re-melting the glass or vaporizing contamination in the glass	The process actually requires cooling of the glass as it exits the draw iris.
Can the polyimide melt during FEP extrusion?	No because polyimide does not melt.
Can the in-line diameter sensors detect the depressions and bubbles in the polyimide, which tend to be associated with the “rocket engine” defects?	The laser micrometer system has a range from 0.067-2mm (67 microns-2000 microns) a resolution of 0.0001mm (.1 microns) a repeatability of ±.0.0001mm and a linearity of ±0.001mm. This equipment is not suitable for finding 10 micron sized features.

5.0 INSPECTION TECHNIQUES AND FAILURE ANALYSES

5.1 Optical Inspection

Comparisons of several different measurement methods were accomplished over the course of the investigation. Attenuation meters, optical fault finders (OFF) and optical time domain reflectometers (OTDR) were used as part of the harness acceptance procedure and during failure analysis. A ray tracing analysis was performed by Boeing, which showed that the size, shape and typical location of the defect made it somewhat invisible to an OTDR. "Rocket engine" defects, which did not reach sufficiently deeply into the core, would be even more difficult to detect with a meter measuring transmitted or returned power.

Attenuation measurements were made with a Model CP-1107 Optical Power Tester manufactured by RIFOCS (1300 nm wavelength, +3 to –80 dBm dynamic range) after harness assembly and during their integration into the US Lab module at KSC. A limit of 1.5 dB per link was used by Boeing though most achieved closer to 0.5 dB, which is associated with connector loss. Link lengths on the US Lab are between 10 and 60 ft [ref-5]. After installation, a system level acceptance was imposed based on successful operation of the data bus. The operational margin afforded by the receivers is between 11.5 dB and 26 dB depending on the type of system (audio or visual) it is part of. Changes in link attenuation associated with degrading fiber may not be discernable using a system test.

Optical fault finders (OFF), which launch < 1mW of red light into the fiber core, were also used to find breaks. The FEP and Teflon™ strength members are transparent to this wavelength and revealed a glowing spot where light was escaping from the fiber through a break or other defect that reached into the core. Research has shown that operators must be dark adapted (@ 20 minutes in a completely darkened room) to effectively use OFF's. Experiments at GSFC showed that several of the defects believed to be "rocket engine" defects, were not found with an OFF until the screen was done following dark adaptation. By using a green laser (< 1 mW, 532 nm, class II), visual sensitivity is raised by a factor of 10, further improving the efficiency of the screening method. Increasing the power of the laser used will also improve the screen, which was verified using a 20 mW HeNe laser. Screening with the 20 mW laser did not damage the fiber. A maximum power for inspecting this fiber, in this manner, was not investigated.

Optical Time Domain Reflectometers (OTDR) were also used to estimate attenuation and especially to locate the defects. Several different models were used with varying sensitivity due to the type of signal launch each used. The models used were the Tektronics TFP2 FiberMaster and the Opto Electronics Inc. OFM20 and OFM130. BICC uses a Tektronix TFP2 FiberMaster and a GNNettest CMA 4000 at 1300 nm [ref-6]. The GNNettest was not evaluated with a length of cable with known "rocket engine" defects. The OFM130 was determined to the best of the three evaluated because it has a zero meter dead zone and a 0.1 μsec pulse [ref 7]. The OFM130 was able to identify the location of more defects than the FiberMaster. Following screening with an OFF, which found yet more defect sites, the OFM130 was applied. By increasing the OFM130's gain to close to its maximum level and scanning the cable at the positions identified by the OFF screening, all of the defects were found.

It is clearly more labor intensive to locate the "dim" spots using only an OTDR. All three OTDR models were also found to show ghost pulses when used with concatenated harnesses. Time and the availability of experienced OTDR operators are required if the OTDR is to be depended on for a screening method for these defects. A Brillouin OTDR was suggested for use but would not be suitable here because its operational mode does not allow the sensitivity required.

5.2 DPA Results

Destructive Physical Analyses (DPA) were done when multiple defects were being found following periods where no stress was induced on the cable (glows appearing after the cable sat on the bench overnight). Most of the early DPA's were done on fiber ends and glow spots on the fiber that had not broken into two pieces at a defect site. When a glow was found in the cable, the affected section was cut from the spool or harness and the fiber was removed from the cable. Often, the fiber broke during this removal operation. When it didn't, the fiber was sometimes bent until a complete break occurred. In either case, the break always occurred at the defect site. The end face images were not mirrors of each other indicating loss of material during the break. As the investigation progressed intact fiber with defects were imaged.

Figure 1 above is one of the very first images of a rocket engine defect made available by Boeing-HB. Subsequent DPA's found other important features, which ultimately led to the HF etching theory. These are shown in Figures 5 through 10.

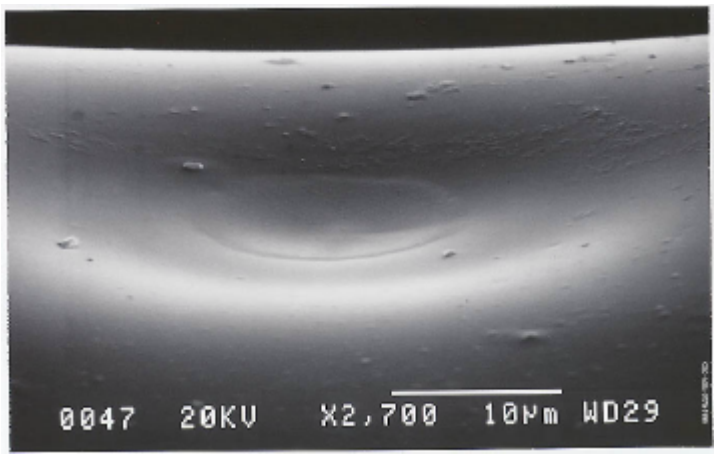

Courtesy of The Boeing Corporation

Figure 5 Sink in the Polyimide Coating

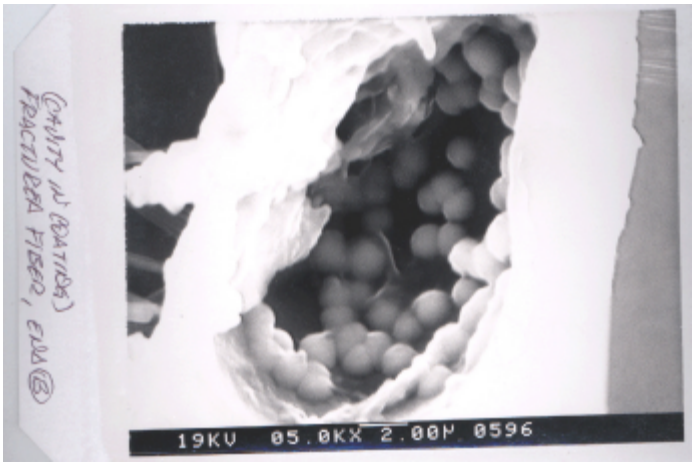

Courtesy of The Boeing Corporation

Figure 6 SiO2 Balls in Polyimide Void

a.

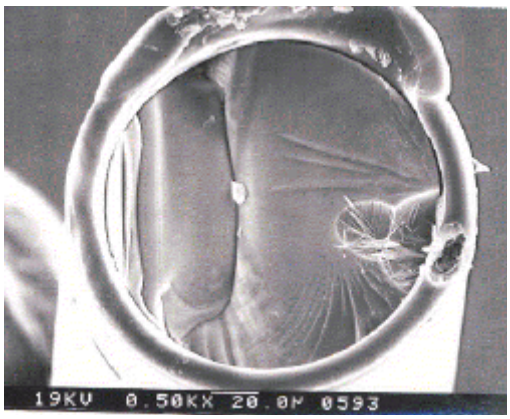

Courtesy of The Boeing Corporation

b.

Courtesy of The Boeing Corporation

Figure 7 GeO2 Crystals in Etch Pit

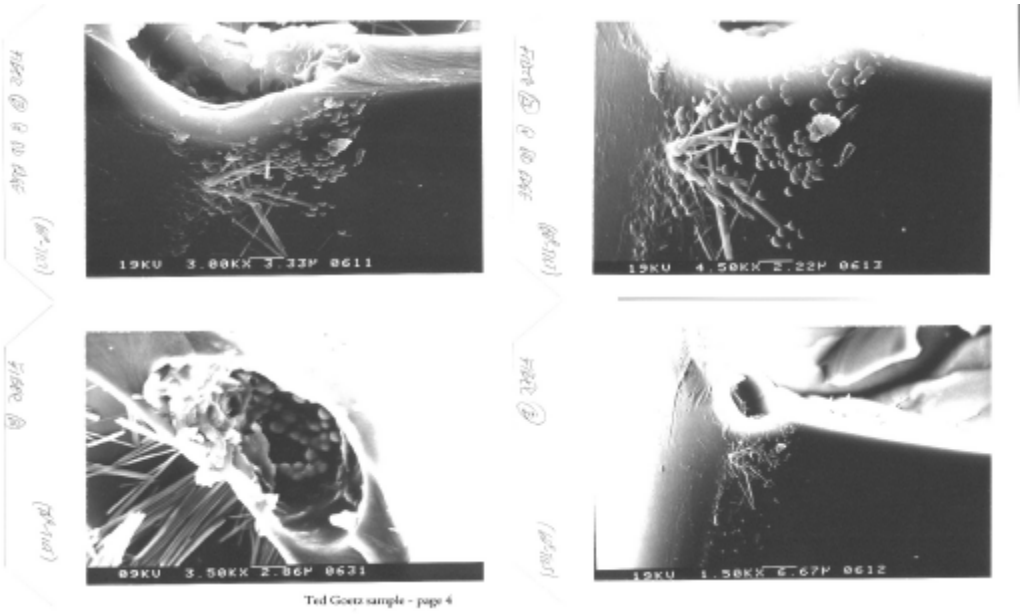

Courtesy of The Boeing Corporation

Figure 8 GeO2 and SiO2 Debris on Outside of Coating

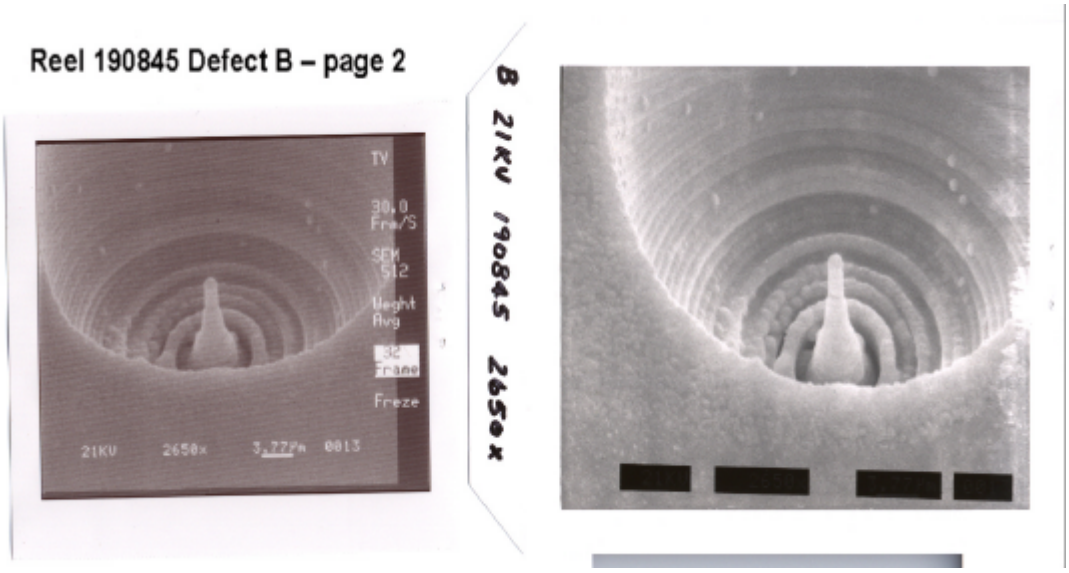

Courtesy of The Boeing Corporation

Figure 9 Si-spire in Deep Etch Pit

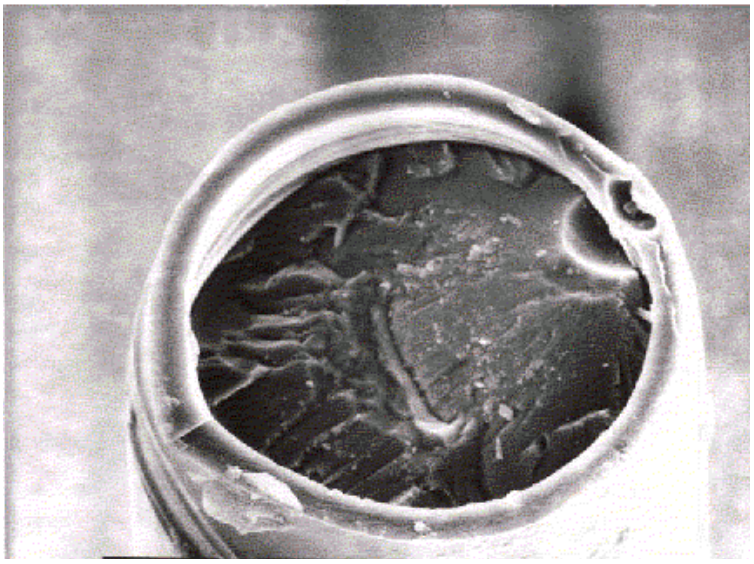

Courtesy of The Boeing Corporation

Figure 10 Characteristic Void in Polyimide Above Shallow Etch Pit

These figures were all produced with a scanning electron microscope. EDX was used to determine the composition of the glass to determine the presence of contamination and to identify the composition of the spheres and crystals found in Figures 6 and 7. Polarized light was used to confirm that the "shards" were indeed crystalline. Optical microscope images are also available but are more difficult to interpret independently.

The use of index matching oil and backlighting during imaging was found to greatly enhance the optical microscope images. After submersion of an intact piece of fiber in index matching oil and having left the sample overnight, the oil was found to have filled the "rocket engine" void (Figure 11a and 11b). This indicated that the surface of the "rocket engine" defect was exposed to ambient atmosphere.

a. b.

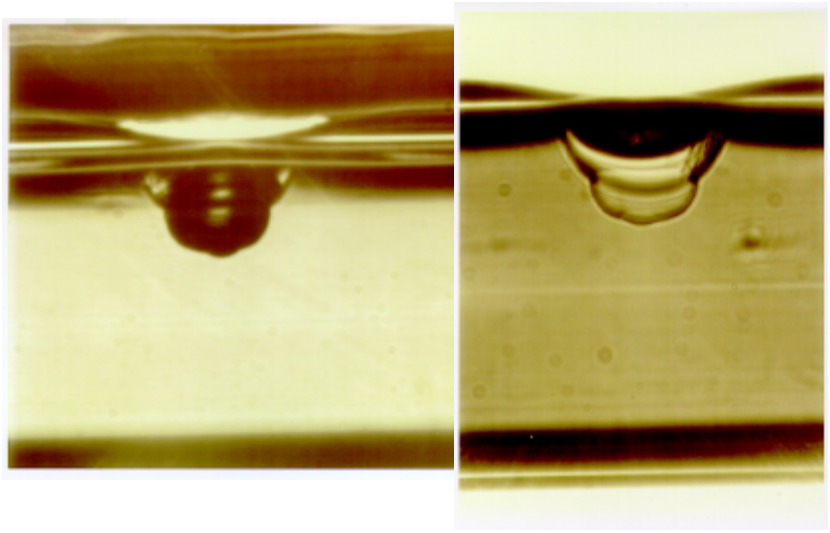

Courtesy of NASA GSFC

Figure 11 Defect Inspection Using Index Matching Oil

Optical inspections were also performed on a section of fiber with no "glow" spots which was taken from a cable with many "glow" spots in other locations. This review showed that the "rocket engine" was not the only observable defect but that many concave "sinks" were found in the polyimide and were believed to be bubbles or indicative of smaller "rocket engine" defects which did not reach beyond the cladding into the core of the fiber. The frequency of these additional defects was one every three to four millimeters (4 to 6/inch).

Optical inspection was used to examine the polyimide surface of fiber containing "glows". Features were found resembling depressions and buried bubbles (Figures 5-8, 10, and 12). Field emission scanning electron microscope (FE-SEM) inspections were also performed on 6" samples from two lots of fiber which had never been cabled by BICC (Figure 13) [ref 8]. The samples were from reels CD0588XD and CD0384XB. Though both lots were found to weaken due to the cabling processes, the CD0588XD fiber was found to be more dramatically weakened than the CD0384XB (see Section 7.0). Sixteen features were found in the polyimide in the "588" sample and one was found in the polyimide in the "384" sample (four more features were found in an additional sample of "588" fiber). An hour glass-like shape was found to be very common among the bubbles observed, as is shown in Figure 13.

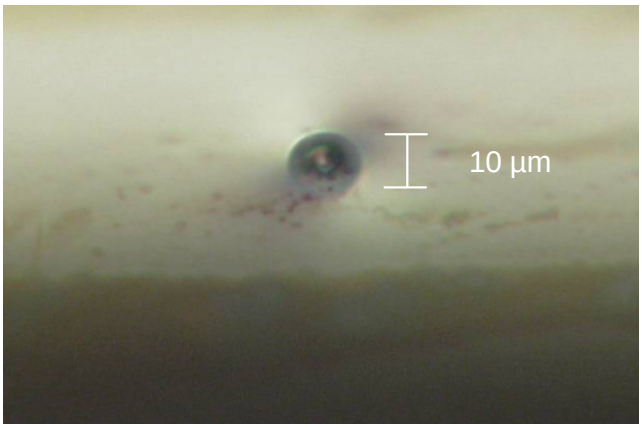

Courtesy of The Aerospace Corporation

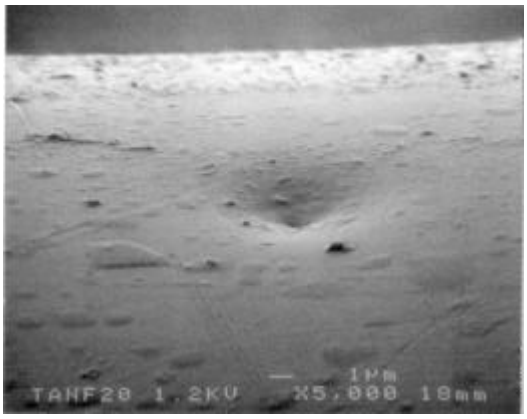

Courtesy of The Aerospace Corporation

a. OPTICAL *b. FM-SEM, 60° to Normal to Surface*

Figure 12 Depressions and Bubble in Polyimide Coating in Fiber CD0588XD

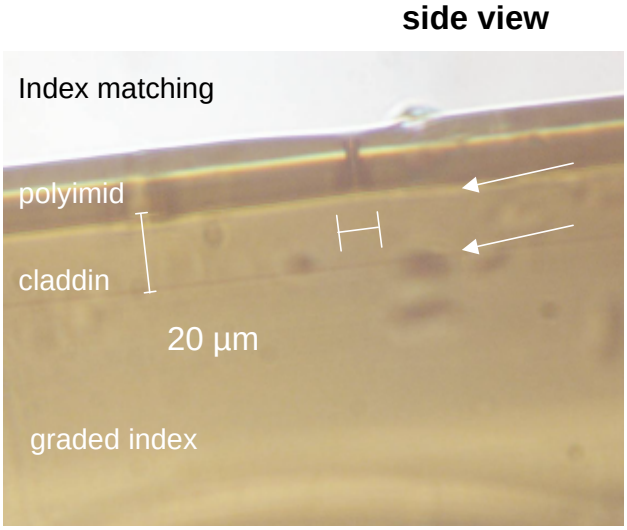

Courtesy of The Aerospace Corporation

Figure 13 Hourglass Shape of Bubble and Polyimide

The arrangement of the bubbles and depressions were found to be in a fairly straight line and parallel with the longitudinal axis of the fiber. Figure 14 is a plot of the distribution of the features along the length of one of the "588" samples.

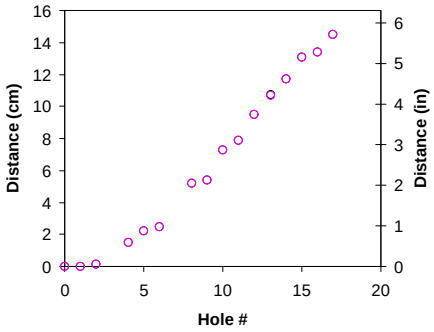

Figure 14 Distribution of Features Along a 6" Sample of CD0588XD Fiber

Additional work with these samples was done to catalogue their relationship to breaches in the carbon coating below them. Not only were breaches found below some of the bubbles, but others were found in the vicinity of the bubbles but with no bubble on top of them as seen in Figure 15a and b.

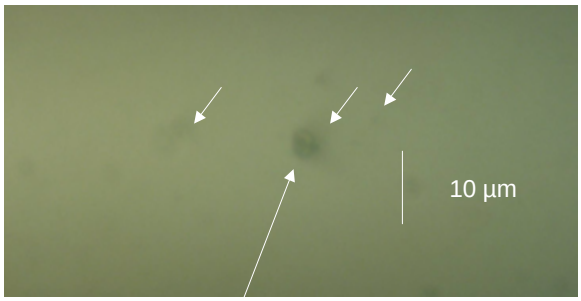

Courtesy of The Aerospace Corporation

a. Features Below Polyimide Bubble, Reflection Mode 100x, 0.3 mm Resolution

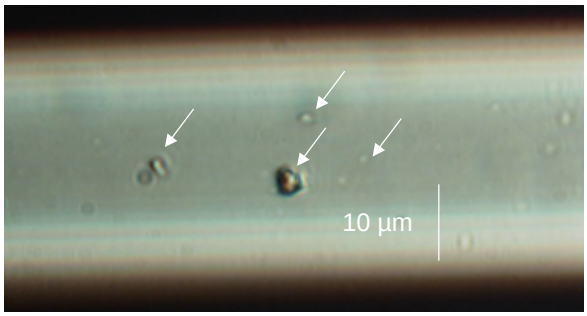

Courtesy of The Aerospace Corporation

b. Polyimide Etched off with Sulfuric Acid, Multiple Bright Spots at Carbon Coating Surface, Transmission Mode

Figure 15 Carbon Defects Seen Below Polyimide on Sample of CD0588XD Fiber

X-ray was used to see if defects on the surface of the coated fiber could be detected. Figure 16 shows that X-ray can be used to look at the fiber without removing the cable elements which is useful for inspecting for fiber which may be too long for the jacketing (in cases where the jacket and/or buffer has shrunken).

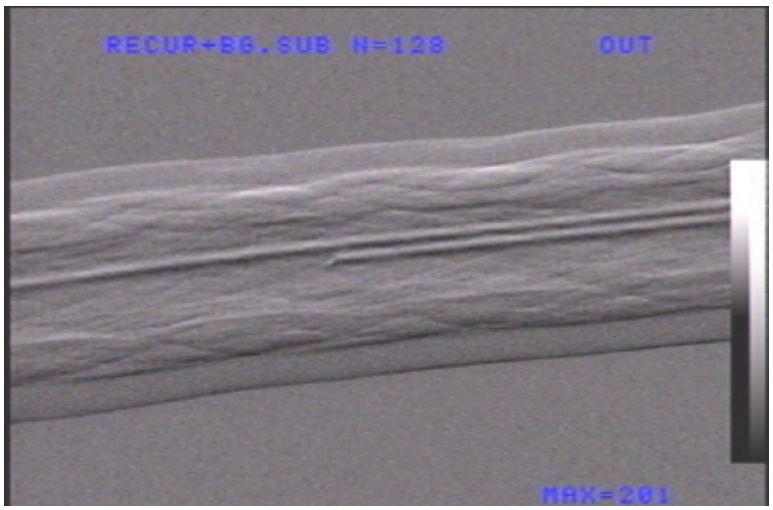

Courtesy of The Boeing Corporation

Figure 16 E. Banks' Sample With a Broken Fiber Whose Ends Overlap

A fiber inspection system, built by the US Army Aviation & Missile Command for their own internal use, was used to try to inspect for 10 µm sized features in the polyimide surface that might indicate the presence of the bubble feature that has been consistently associated with "rocket engine" defects and low strength breaks. The system uses an infrared detector and looks for signal scatter off of the surface at feature locations. The feature is described with respect to the voltage of the returned scattered signal. When a feature is found that corresponds to a minimum signal voltage, the system takes a picture of the corresponding location. The inspection system is very sensitive to any surface feature, especially contamination such as lint and dust (Figure 17). A lint free dust capture stage was arranged around the fiber and the inspection was continued. Figure 18 shows the image of a debris-free fiber with polyimide surface features.

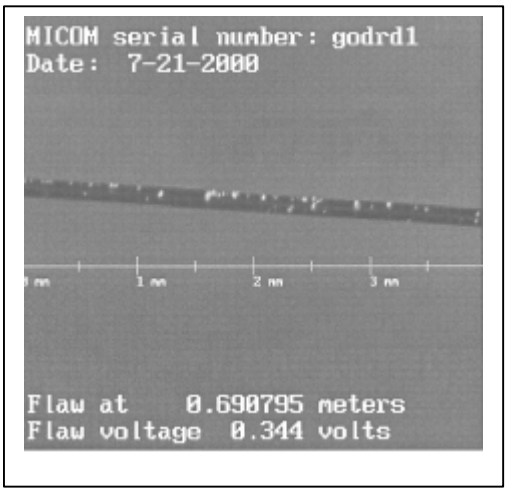

Courtesy of US Army Aviation & Missile Command

Figure 17 Debris-Laden Fiber

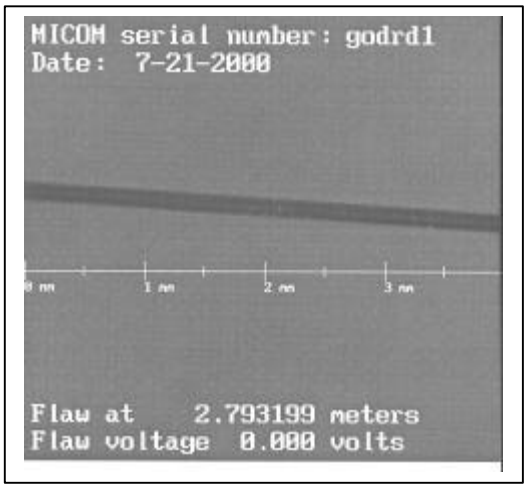

Courtesy of US Army Aviation & Missile Command

Figure 18 Cleaned Fiber

To see if, using a more typical inspections speed, 0.5 m/sec, the machine could provide useful statistics which would differentiate the two reels. Figure 19 and Figure 20 show the results of running approximately 400 m through the machine, looking for a 0.1V feature size or greater. Additional work is required to understand the usefulness of a system such as this to identify defects in the polyimide coating.

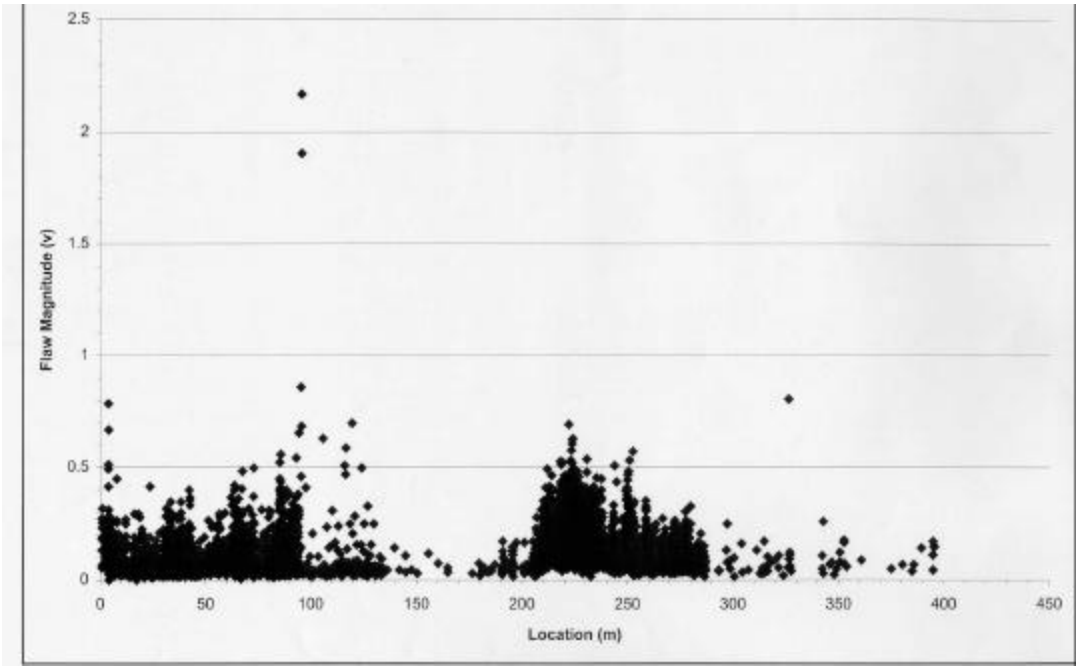

Figure 19 Feature Statistics for CD0588XD

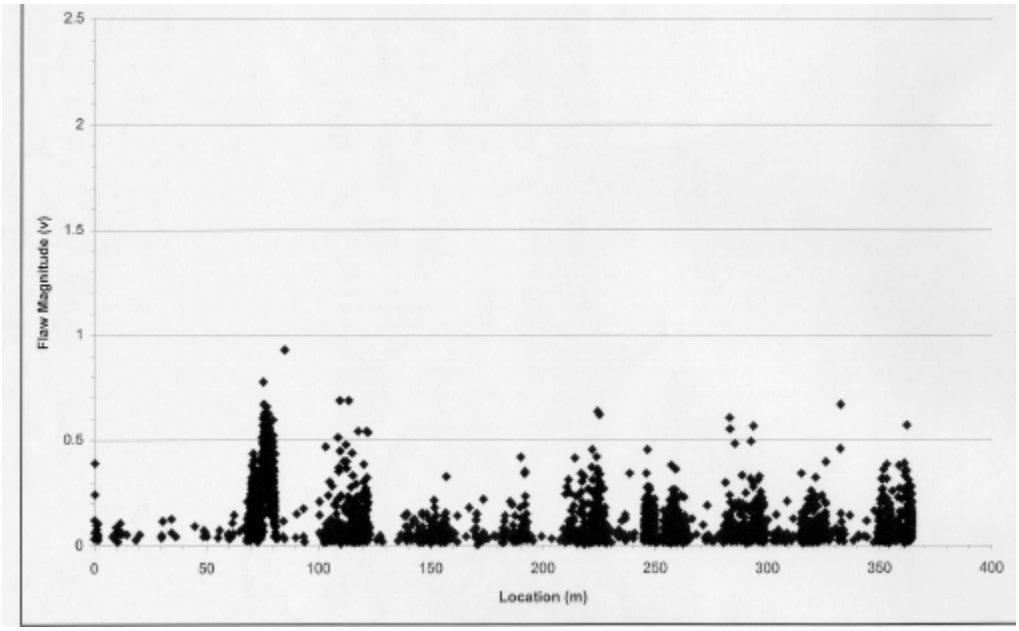

Figure 20 Feature Statistic for CD0384XC

6.0 MATERIAL BEHAVIORS AND INTERACTIONS

The interactions between the materials used for the fiber, its coating, and the cabling components are believed to be at the root of the "rocket engine" defects. These materials were examined, as were their interactions in the environments created by the manufacturing processes. Artifacts found during the DPA's led the investigation team to hypothesize about various material reactions including: decomposition of the FEP buffer, discontinuities in the carbon/polyimide fiber coating leaving the glass exposed to etchants and moisture, the electrical properties of the carbon/polyimide coating and the thermal stability of the polyimide layer.

6.1 FEP Decomposition

FEP is a copolymer of tetrafluoroethylene (TFE) using hexafluoropropylene (HFP). It is sometimes generally described as a Teflon® however its properties and processing requirements can be very different than those of the homopolymer PTFE. FEP is applied in optical cable manufacture using a melt extrusion process. The maximum service temperature for FEP is 206°C (400°F) and the maximum processing temperature is 400°C (746°F). The temperatures used in the BICC General process extend close to the maximum processing temperature.

Decomposition of FEP depends upon the composition and temperature of the ambient environment. In a moist or dry environment containing oxygen, FEP decomposes at a rate of 0.05% and lower, by weight, below 325°C (612°F) and at a rate of 2.5% and higher, by weight per hour at 400°C (746°F) [ref 9,10, 11]. In a moist or dry nitrogen environment the decomposition rate at 400°C (746°F) drops to 0.40%/hour. When the atmosphere contains oxygen, the decomposition product is mainly COF_2. In a dry, nitrogen atmosphere COF_2 is not created.

Though the COF_2 was the majority decomposition component measured by Baker and Kasprzak, they noted that it was difficult to capture all of it in the measurement because it so rapidly reacts with air, water and the quartz chamber the FEP sample was heated in. Baker and Kasprzak remind us that at the temperature and humidity (50% RH) of their experiments COF_2 "hydrolyzes considerably according to:"

$$COF_2 + H_2O = CO_2 + 2\ HF \qquad (1)$$

Testing was performed by NASA GSFC to confirm the evolution of reactive, fluorine containing gases, such as HF or COF_2 from the NFOC-2FFF-1GRP-1 cable due to mechanical agitation and exposure to an electric field. The set-up is shown in Figure 21. The NFOC-2FFF-1GRP-1 cable and OC1260 cable were tested. The OC1260 cable uses the same cable materials as NFOC-2FFF-1GRP-1 except that its optical fiber does not have the carbon layer under the polyimide coating. In both cases, the length of cable was hooked up to a mass spectrometer. After pumping out all the gasses for between 16 and 72 hours, the cable was stressed in the two different ways, mechanically twisting and exposure to an electric field.

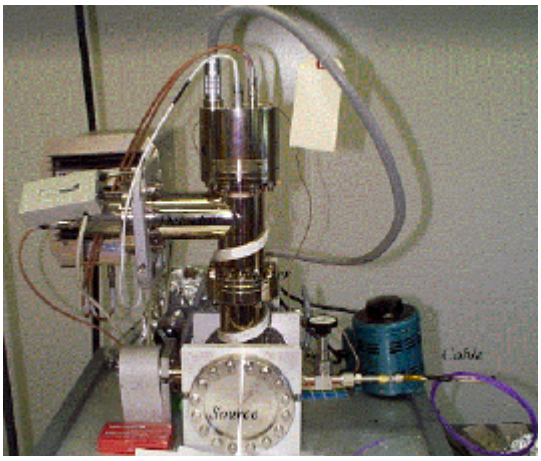

Courtesy of NASA GSFC

Figure 21 Set-up for Mass Spectrometer Measurements of Fluorine Species Released From Fiber Optic Cable

Mechanically twisting the NFOC-2FFF-1GRP-1cable resulted in the release of fluorinated species that persisted for about five minutes. Mechanically twisting the OC1260 released three orders of magnitude less Fluorine. The spark from a Tesla coil was run over a length of the cable to induce charge breakdown by the cable components and the polyimide coating ending at the grounded carbon coating in the NFOC-2FFF-1GRP-1 cable. This condition also resulted in a release of fluorinated materials, in larger quantities, lasting again about five minutes. In the case of minimal air leakage into the cable, a longer distance between the spark and the mass spectrometer corresponded to a lower mass flux rate from the cable and a longer mass flow. After 48 hours, a significant fraction of the gasses entering the mass spectrometer was water.

6.2 Polyimide Related Issues

The polyimide coating is intended to protect the fiber from mechanical insults. Its operating temperature range allows it to perform this function from -269°C (-452°F) to 400°C (752°F). This range makes it suitable for use by ISS external vehicular applications where coating materials normally used for commercial applications would fail. The polyimide coating also plays a role with respect to damage that may occur to the carbon layer and the glass when the fiber is exposed to a static electric field and how HF generation may be occurring. DPA's of the "rocket engine" defects showed that the polyimide layer at these defect sites often contains a void (Figure 7). It is not known how these voids occur, though they are consistently associated with the rocket engine defects, and the low strength defects. They have been found in coated fiber obtained directly from Lucent-SFT indicating that they are created prior to shipment and processing by SEA or BICC. Their root cause and their role in the reduction of fiber strength following the many processes used at BICC is not yet understood.

The polyimide is applied to the fiber through a polymerization process, not a melt process. DuPont's recommendations for fully polimerizing polyimide could not be located. We were however, able to find the glass transition temperature (Tg =325°C,), the dielectric withstanding voltage (DWV = 4 kV/mil) and the modulus of the material used on this fiber (245 kg/mm^2) [ref 12]. Polyimide should not melt when its glass transition temperature is exceeded. Lucent-SFT does not exceed the Tg when it processes the polyimide coating. Though Lucent-SFT utilizes cure temperatures that are recommended by DuPont to drive off the solvents, the rapid travel speed through the cure ovens may not allow complete solvent outgassing.

Polyimide's hygroscopic nature provides a sink for ambient H_2O. This H_2O can, in the presence of COF_2 at room temperature and above, result in the creation of HF during manufacture of this cable. COF_2 and HF can diffuse into polyimide. Polyimide will act as a sink for HF as it does for H_2O. Diffusion of HF into and within the polyimide will continue until equilibrium is reached. HF will diffusion into some species of carbon and not into others. If the amorphous carbon layer directly under the polyimide has a species, such as carbon black, which absorbs HF, then the carbon black will be part of the equalibrium dynamics. Some species of carbon do not absorb or react with HF and so will not be part of the HF sink. Bare SiO_2 or GeO_2 react with HF and so, are also part of the HF sink in the polyimide/carbon coated glass system. The HF will diffuse into the polyimide as long as there is more HF outside of its outer diameter than there is inside of its volume, plus the volume of the absorbing carbon species plus the amount not yet consumed at the bare glass interface.

Polymers used in electronic packaging have been tested to identify the risks associated with trapped water when the part is suddenly exposed to high temperatures, such as happens during soldering [ref 13,14]. Plastic encapsulated microcircuits have been found to fail due to delaminations at the plastic-to-metal lead frame interface when the trapped water expanded. These type of failures, known as popcorning, were found to occur at material interfaces rather than within the homogeneous material, even if voids were present. Better adhesion of the materials by the use of a primer or by roughing the surfaces is reported to be possible solutions for reducing water collection at these interfaces. Popcorning as a root cause has not been investigated as of the date of this report.

The final thickness of the polyimide on the BF04515 is 15 μm (0.60 mils). The cure schedule used may make its mechanical and electrical characteristics differ from DuPont's published values [ref-12]. The polyimide coating on a sample of BF04515 fiber, which had never been cabled, was tested for dielectric strength. Several lots were not tested so we do not know how the value may vary on a lot basis. A value of 6.5 kV/mil in 50% humidity [ref-15] was measured (See Section 6.5 below for the test set-up and more discussion about ESD testing). DuPont's published value for fully cured polyimide is 4.0 kV/mil at 50% RH. Burn marks were found on the sample tested (Figure 22).

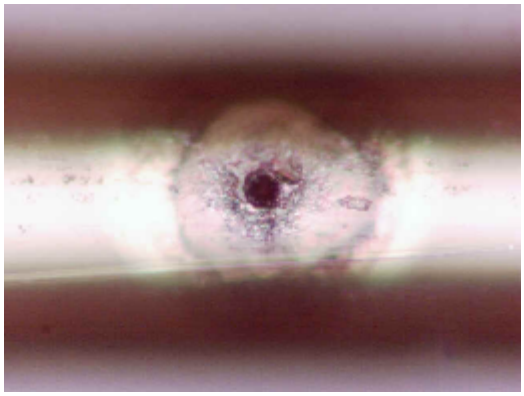

Courtesy of The Aerospace Corporation

Figure 22 Burn Mark From DWV Testing of "Rocket Engine Defect"- Free Fiber

Another test was done on fiber that was removed from NFOC-2FFF-1GRP-1 cable that was known to be defective (several "glows" found along its length, at least one of which was DPA'd and found to be a "rocket engine"). A voltage of 1.5 kV was enough to break through the polyimide between two electrode locations and sustain a current down the carbon coating between them. A burn-mark was created when the voltage was raised to 2.5 kV (Figure 23).

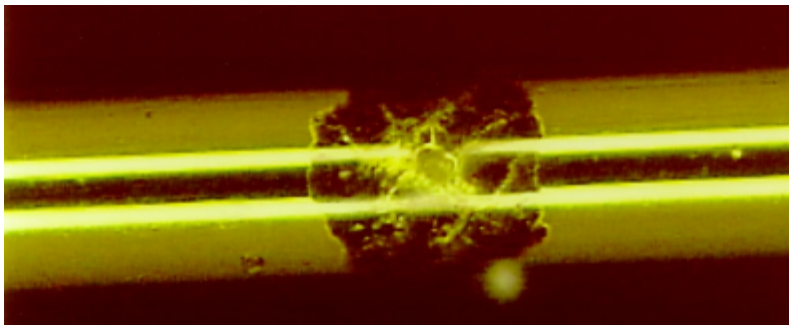

Courtesy of NASA GSFC

Figure 23 Burn Mark From DWV Testing of Fiber with "Rocket Engine Defects"

6.3 HF Etching

HF is known as a "weak" acid. It is not significantly ionized in water. As such, it is not reactive with polyimide or most other organic materials. However, due to the polarity and hydrogen bonding characteristics of HF, it has a tendency to absorb readily into and coordinate with the polyimide. Analogous to polyimide's tendency to retain water, HF is also retained by the polyimide. The polyimide acts as a sink for the HF. When HF becomes part of an etching reaction, more HF is delivered from the surrounding polyimide to the etching site in order to maintain chemical equalibrium.

Hydrofluoric acid is a well-known etchant of glass. The reactivity and reaction product of hydrofluoric acid with glass was first described in a scientific journal in 1771 by Scheele. The formation of germanium tetrafluoride was documented by C. Winkler in 1886. The formulas describing the reaction in the Ge doped fiber are:

$$4\ HF\ (g) + SiO_2\ (s) \leftrightarrow SiF_4\ (g) + 2\ H_2O\ (l) \quad (2)$$

$$4\ HF\ (g) + GeO_2\ (s) \leftrightarrow GeF_4\ (g) + 2\ H_2O\ (l) \quad (3)$$

The oxides are solid and ordered in the original fiber structure. Mechanistically, the reaction of hydrofluoric acid with a silica surface (or in similar manner with a germania surface) first requires the insertion of water into a silicon oxygen bond. This insertion hydrates the silica, providing a readily exchangeable group to react with the hydrofluoric acid. This step of the reaction is controlled by the activities of the hydronium ion and the silica surface. As the silica is hydrated, the hydroxyl groups present on the silica are replaced with fluoride groups in an extremely exothermic reaction. The rate of the reaction is dependent upon the equilibration of a wide variety of species both as the products and the reactants. Due to the complexity of the reaction, there have been few or no definitive studies of the reaction of HF with siliceous materials in spite of the great interest and long time elapsed since the discovery of the reaction.

Silicon and Germanium fluorides are gases and take up almost 840 times more volume than the oxides, possibly causing a pressure "eruption" of gases out of the orifice. The gas phase nature of the reaction products provides for rapid mass transport of the products from the reaction sight. This minimizes the build up of reaction products that could result in slowing of the reaction. The gas phase reactants will also react in the reverse reaction at a significantly higher rate due to the faster mass transfer rate. Additionally, the

reaction creates heat in the forward direction, adding to the force of the eruption. The ejected material is SiO_2 and GeO_2. The escaped fluoride gases, in the presence of water, will be in equilibrium with SiO_3H_2, GeO_2 and HF; this is essentially the reverse of the reaction proceeding from the point of the protonation of the glass surface. This regenerates the HF in a catalytic manner. There are some side reactions that may slightly decrease the active HF concentration; however, the HF is recoverable for reaction with the glass until the HF is physically removed from the system. The SiO_2 precipitates as a silica gel when the water around it evaporates giving rise to spherical shapes surrounding the hole. The spheres are silica in a hydration state, but not vitreous glass. The same occurs for the GeO_2, except that it forms a shard-like crystalline structure. The reaction conserves mass and energy.

The shape of the cup in the cladding area reflects the speed at which the reaction occurs in the pure silica material and its increasing speed in the Ge rich material. A FEA model was constructed for the BF04515 fiber to understand the internal stresses in the glass with a "rocket engine" defect when the fiber is under a 25% strain (Figure 24a through c). Figure 25a through c shows that the internal stress in the fiber in this case rises by a factor of three over a section, which is experiencing the same amount of strain with no "rocket-engine" defect.

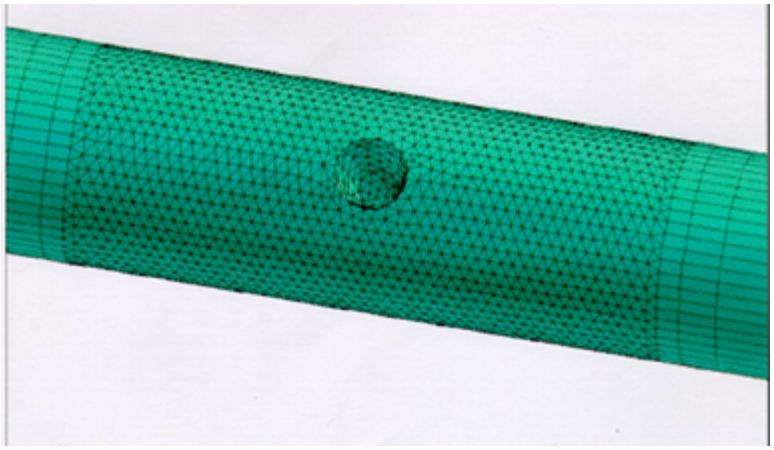

a. Element Mesh of Flawed Fiber Geometry

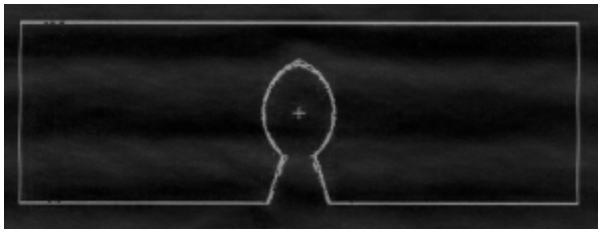

b. Side View of "Rocket Engine" Defect

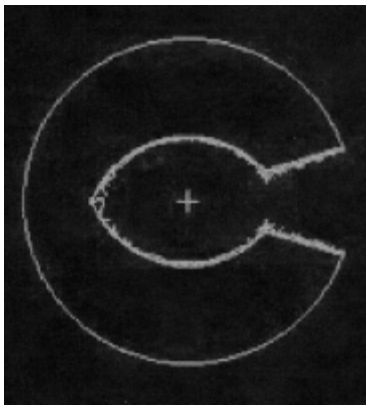

c. Crossectional View of "Rocket Engine" Defect

Figure 24 Model of "Rocket Engine" Defect

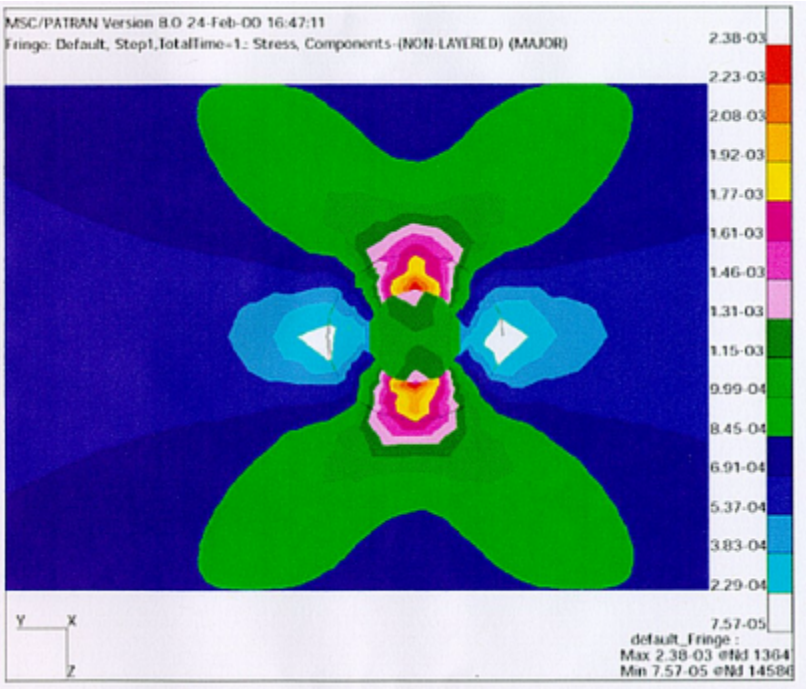

a. Stress in Flawed Fiber Under 25% Strain (view from top looking down into the hole)

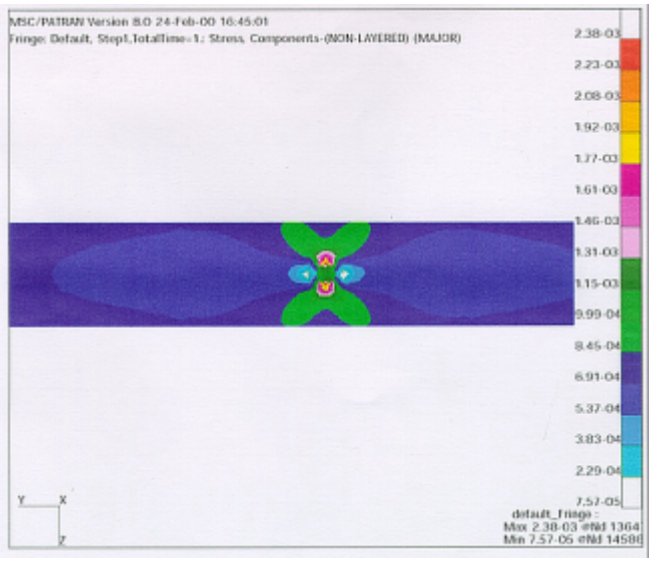

b. Top View of Stress Model

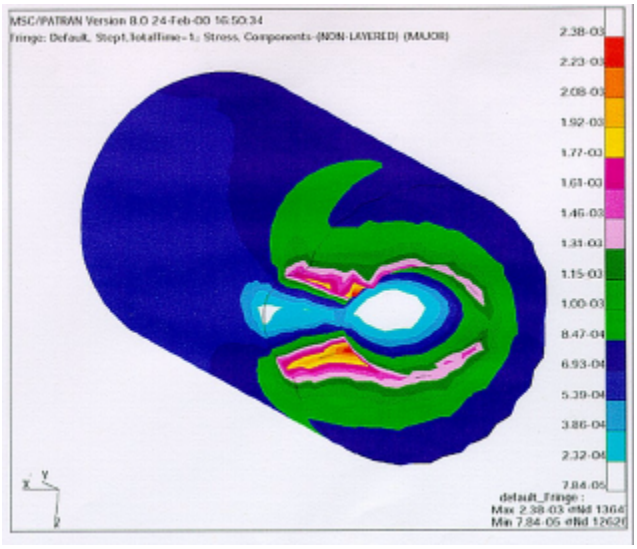

c. 45° Cutaway View of Stress Model

Figure 25 Stress Predicted by Fiber Model

Lucent Technologies experimented with BF04515 fiber from a cable with “glows”. The polyimide coating was stripped and the grounded, carbon coated fiber was exposed to a 1 kV source (wire electrode). An arc discharged through the air between the wire and the fiber. The sample was then exposed to both aqueous and vapor HF (in a humid environment) [ref-16]. HeNe light was transmitted through the fiber during the test and when light began to leak out of the side, the test was stopped. Figure 26 shows the resulting defect with the characteristic bulb pattern and ringed structure seen in the Boeing photographs (Figures 9). The sample was rinsed to drive off the highly corrosive HF, so it is not known whether there were any GeO_2 crystals or SiO_2 balls resulting from the experiment.

Lucent observed that the Ge-doped core etches considerably faster than the cladding. If the etch time is too long, then the entire core can be removed, leaving a silica tube with a pinhole in it. This indicates that the amount of HF present at the site is the limiting factor in the degree of etching.

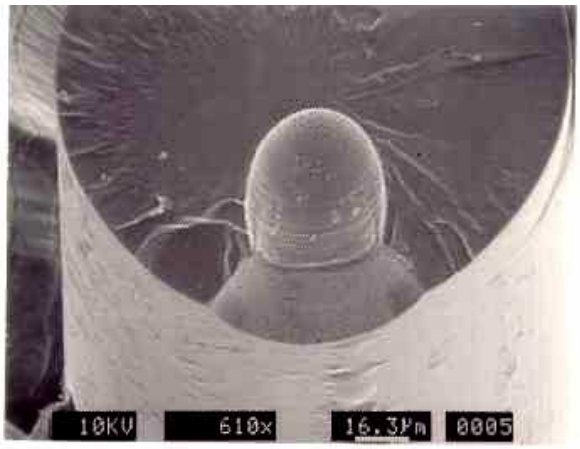

Figure 26 Etch Pit Resulting From Experimentation

Experiments were performed on 2 inch long samples of fiber removed from NFOC-2FFF-1GRP-1 cable and exposed to the vapor over liquid HF. Some of the samples had been exposed electrostatic discharge from a Tesla coil, that breached the carbon coating in small discrete points. The polyimide was removed from one half of the sample and left in place on the other half. The entire sample was exposed to HF in a liquid form for approximately 36 hours. The samples were monitored throughout the test to look for the evolution of etch pits at the induced carbon breaches. The glass was found to be etched through the pin-holes and through the endfaces of the fiber. The etching on the end without the polyimide continued into the carbon/polyimide coated section and the carbon left behind fell to the bottom of the fluid. The glass was also etched from the endface of the carbon/polyimide coated half but there was not sufficient time to allow the etch to occur past the end of the polyimide coated section. A control sample of fiber taken from OC-1260 cable with acrylic coating showed similar results in the half where the coating was left in place, however it showed a necking down of the glass from the outside in the uncoated portion of the fiber from contact with condensing HF. This showed that the carbon protects the fiber from HF attack when it is continuous.

6.4 Carbon Layer

BF04515 fiber is coated with a 25 nm coating of carbonaceous material which is intended to serve as a hermetic coating which increases the fiber’s strength and increases its reliability. Lindholm, Li et al. [ref-17] performed reliability studies with Lucent-SFT carbon coated fiber and found high strength associated with various thickness of carbon on fiber. The carbon is deposited pyrolytically as the fiber exits the draw furnace. A mixture of hydrocarbon gases enters into a chamber in the presence of a nitrogen purge. This then cracks the hydrocarbons onto the surface of the fiber. Some of the carbon species lumped into the

"amorphous carbon" group are electrically conductive and others are not. Some act as a diffusion barrier to HF and some absorb HF and act as a catalyst in etching reactions. The species of carbon, which result on the surface of the quartz cladding and their order, is not completely understood.

Breaches in the carbon coating allow the "rocket engine" defects to occur when the environment around the exposed glass contains HF. They also allow moisture corrosion of the exposed glass. Finally, when large enough, they can be located by observing light, which escapes out of the fiber through them.

During examination of the polyimide surface and the bubbles in the polyimide, a 6" sample of fiber from lot CD0588DX was believed to have a carbon breach below a prominent bubble. The polyimide was removed with sulfuric acid, which is not damaging to the carbon. Not only was a light emitting breach found below the bubble site, but companion breaches were found around it and were not associated with prominent bubble-like features. A better understanding of the molecular structure of the carbon created by Lucent-SFT's process will allow exploration of the process or handling conditions which cause breaches in it and leave the glass exposed to etchants such as water and HF. [ref-18]

6.5 Electro Static Discharge (ESD)

Respooling processes used on uncabled fiber by Lucent-SFT and BICC, are believed to expose the cable to significant levels of electrostatic charging, which when discharged, may damage the fiber coatings.
To understand the signs and magnitudes of the static charges present around the "color line" used to respool fiber at BICC, measurements were made with ESD meters (see http://misspiggy.gsfc.nasa.gov/tva/library/essays.htm for background on static charges). The values measured are presented above in Table 4. Measurements of the field strengths at several spots in the fiber draw and coating process at Lucent-SFT were similar to those measured at BICC. The respooling process at SEA was not reviewed because they do not handle uncabled BF04515 fiber.

Dupont's value for the dielectric breakdown field strength for the polyimide used by Lucent-SFT is 4 kV/mil for a 1 mil sample, at 50% relative humidity. This number will decrease at 100% and increase at 0% RH, however those values were not provided in the reference used. The thickness of the polyimide coating applied to the BF04515 fiber is 0.60 mil, thus the dielectric breakdown voltage of the coating should be at least 2.4 kV. The polymerization process used by Lucent-SFT and the presence of thinned spots at bubble sites makes it difficult to predict what level of charge will cause an ESD event terminating at the conductive carbon layer.

NASA GSFC performed a test using the set-up shown in Figure 27a to measure the breakdown strength of a sample of fiber with known flaws. The electrodes were applied between various sets of foil contacts. A breakdown strength of 2.5 kV was measured and a burn mark resulted. The burn mark was found very close to polyimide bubbles (Figure 23).

The Aerospace Corporation used the set-up shown in Figure 27b with an associated burn mark shown in Figure 22. The Aerospace Corporation found abrupt breakdown at 3.9kV in a 50% relative humidity environment, indicating a 6.5 kV/mil dielectric strength. Burn marks were found with a variety of sizes the smallest being 30 μm in diameter. They also measured the resistance of the carbon coating for lengths between 1 and 34 cm to be approximately 15 kOhm/cm, which agrees with Lucent-SFT's databook value.

a. GSFC Set-up

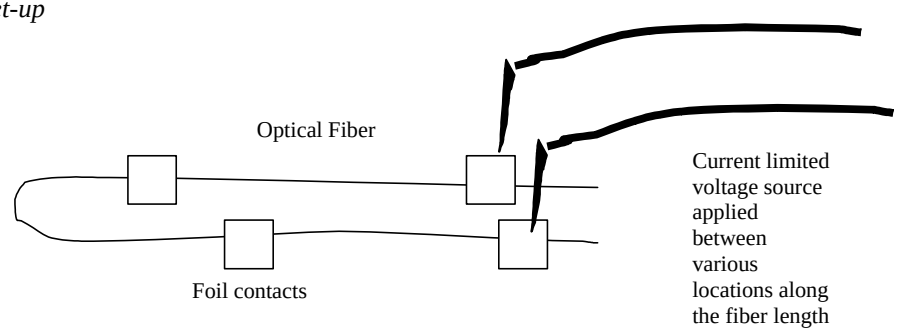

b. Aerospace Corporation Set-up

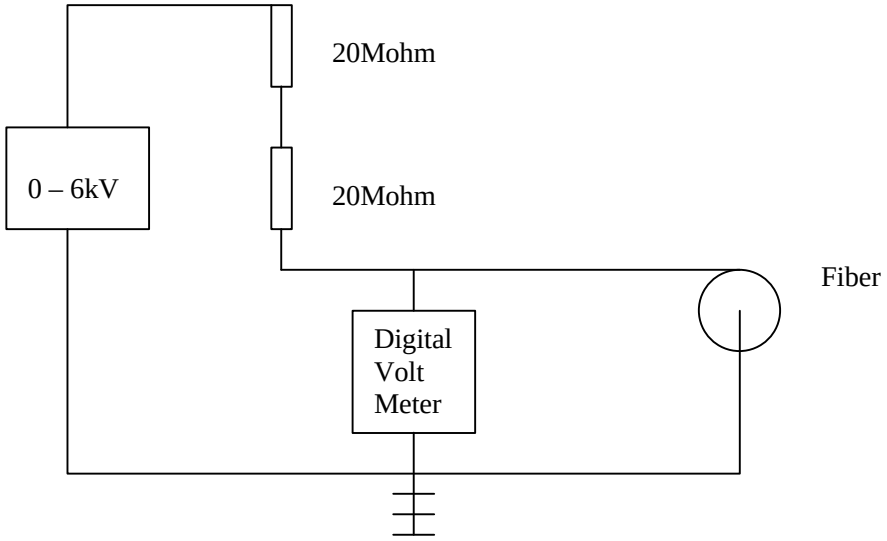

Figure 27 Experimentally Produced ESD Damage

Testing was also done with a 30 kV Tesla coil to demonstrate the conducting behavior of the NFOC-2FFF-1GRP-1 cable. When the Tesla coil tip was placed about a centimeter from the cable, the tip of the coil emitted a spark that was drawn to the cable. This spark was drawn along as the tip of the coil was moved along the cable. Upon removal of the fiber from the cable sample, the trench shown in Figure 28 was observed. Though it is not obvious in the photograph, particles believed to be polyimide surround the blackened edges of the trench suggesting that all of the polyimide did not vaporize and some of it was redeposited around the site near the trench. This demonstrated that high electric fields can cause charge travel all the way through the cable layers and damage the fiber coating.

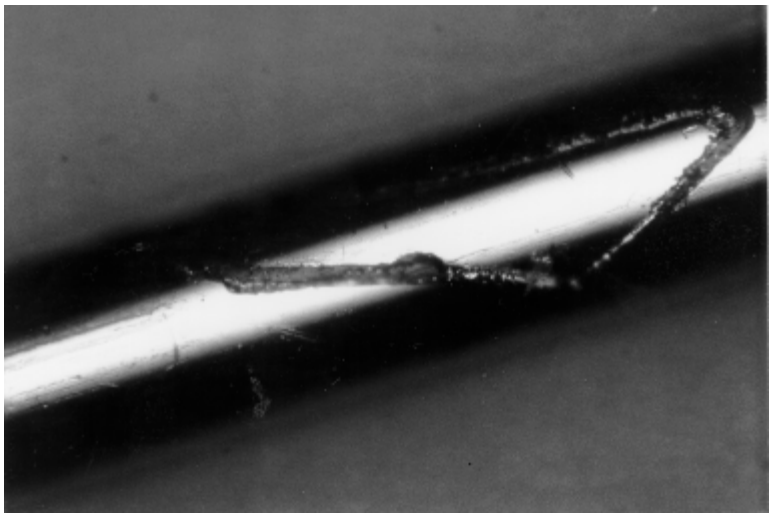

Courtesy of NASA GSFC

Figure 28 Electrical Discharge Induced Damage on Fiber Surface

Another run of this test was performed on 1996 vintage cable and the spark was found to “stick” to a particular site until the coil was move sufficiently far away and then the spark would move with the coil tip. This behavior was not investigated further. The wider portion of the trench seen in Figure 28 may be demonstrating the results of such a “sticking” behavior.

The Tesla coil test was run again using BICCGeneral’s OC1260 product, which contains an acrylate, coated fiber with no carbon layer. This cable was found to be electrically inactive. No spark was drawn from the coil even when the tip was closer than one centimeter to the cable. When the test was done with the OC1260 cable on a table, the spark went around the cable to find the grounded, conductive table.

6.6 Aeolian Motion – Vibration of Fiber Under Tension

When a steady flow of fluid passes an obstacle with a large enough speed, it is usually found that eddies are formed behind the obstacle. Such effects are familiar in the case of a stream of water "swirling" past a rock. Similar effects are also produced in a stream of air. A cylindrical obstacle, such as a rod or wire, in a stream of air sets up a double series of vortices [ref 19]. The stream of air past the wire is thus set into transverse vibrations, as alternate left- and right-handed eddies are formed and detached. This results in alternating pressure waves, which can be audible under certain circumstances. An experimental investigation of these vortex vibrations was first undertaken by Strouhal (1878) and later by Kohlrausch (1881). The frequency "f" of the tone in the air was independent of the length of the wire and also the tension of the wire, and varied only with the thickness "d" and the speed "s" of the wire through the air:

$$f = 0.185\ (s/d) \qquad (4)$$

The detachment of the alternating vortices, and the wavering of the stream of air, produces an alternating transverse force on the wire, which sets it into forced vibration at the frequency "f". We have a pronounced resonance when this frequency coincides with one of the natural modes of vibration of the stretched wire,

$$f_\eta = (n / 2*L) * \mathrm{sqrt}[T/m\mu] \qquad (5)$$

where "n" = 1, 2, 3, is the number of loops in the wire between its fixed ends, spaced a distance "L" apart, "T" is the tension of the wire, and "mu" is the mass per length of the wire. This resonance can result in a large amplitude of displacement of the wire.

The music of the Aeolian harp is produced this way. The harp consists of a number of wires of graduated thickness mounted on a sounding board. The wires are all turned to the same low fundamental note, which consequently has a wide range of overtones in the audible region. When a wind moves past these wires, and "plays" it, one or more of these wires will resonate and emit the note of the appropriate overtone. Other examples include the "singing" of overhead wires, the "sighing" and "roaring" of wind in trees, and the "whistling" of wind through tall grasses. [ref 20]

Aeolian motion may be occuring with the fiber in the draw tower. Using equations (4) and (5), one can predict the periodicity of defects which may be coincident with the resonant frequencies of the fiber in tension. The draw speed being known, we can determine that the defects spaced as shown in Figure 14 move past a fixed point at a frequency of 33 to 83 Hz.

$$T = L/S\_fib \qquad (6)$$
$$f = 1/T \qquad (7)$$

S_{fib} = Fiber Draw Speed
L = Spacial Period Between Latent Defects
T = Temporal Period Between Latent Defects
f = Frequency which the Latent Defects Pass a Point

Several aspects of the process including the glass temperature, the viscosity of the polymer in the coating cups and the speed of the capstan contribute to the tension extended to the fiber. An assumption of 4 lbs for the tension is made based on the proof test value of 5 lbs. The mass per unit length of the fiber is calculated as 42.6 mg/m. The distance between fixed points is estimated as 5 m. Equation (5) above, using these values, gives the natural vibration modes occurring at 65, 130, 195, 260 Hz and so on. Equation (4), for a fiber with a 140 to 170 μm diameter, can be used to show that an air speed of 0.7 cm/sec to 0.9 cm/sec would be required to cause the fiber to oscillate with frequencies listed above.

An experiment was done to measure the displacement amplitude for the fiber excited into motion by a shaker. A length of BF05202 (similar to BF04515 fiber was hung from a shaker, and attached to a weight of 5.96 g at its bottom. The total length that was free to vibrate was 60.0 cm. The first mode was at 30.2 Hz, the second was near 60 Hz, the third was at 90.4 Hz, and the fourth was at 120.8 Hz.

The quality factor, judged from decay times and from the full-width between half-maxima, was more than 100 for these modes. When vibrating in the fundamental mode, an amplitude of about a centimeter at the midpoint was easy to observe when the amplitude at the shaker was invisibly small (less than 0.1 mm), and the rest of the fiber was hard to see without a solid light colored background. When vibrating in higher modes, the fiber was hard to see near the "loops" but seemed to be completely stationary at its nodes: a gauge placed near a node would detect little motion. A wind directed sideways across the fiber caused it to oscillate with an amplitude of a few millimeters.

7.0 STRENGTH TESTING

Strength testing was proposed to help Boeing establish a basis for a risk assessment associated with the life of the cable already installed in the US Lab module. The findings ultimately were critically important to the understanding of the latency of the carbon breach as a defect and the prominent role of the polyimide bubbles.

7.1 Initial Testing of '96 Vintage Cable and '99 Vintage Fiber

7.1.1 Test Approach

Fiber which had not been cabled and which had been cabled were strength tested. Fiber, which had never been processed by BICC, was tested before and throughout the cabling process to understand how each step of that process affects the strength of the fiber. The testing was performed in accordance with EIA Fiber Optic Test Procedure 28, EIA-TIA-455-28B, "Method for Measuring Dynamic Tensile Strength of Optical Fiber". The set-up is shown in Figure 29. When the test was run on cabled fiber, as much of the cable was left intact as possible during the test and laser light was used to identify the locations of the breaks inside of the cable. Table 8 shows the gauge lengths and pull conditions used on the various samples. The cable and fiber that was available from which samples were selected, had already been proof tested to 141 kpsi and screened optically for the "rocket engine" defects. This provided some confidence that no large defects of that kind would factor into the strength data. For high strength samples, the breaks were expected to occur between the range of 11.2 to 12.7 lbs, based on the set-up, loading and the intrinsic strength of the fiber (> 450 kpsi). The resulting data would be plotted as a Weibull distribution which was expected to be bi-modal, one slope expected for the high strength breaks and one for the low strength breaks caused by a defect.

Table 8 Strength Testing Samples and Conditions

Uncabled Fiber Lot Number	Date of Mfr	Cabled Fiber Reel Number	Date of Mfr	Gauge Length (inches)	Pull Speed (in/min)	Effective Strain Rate (%)
CD0384X	1/21/99			20 80	0.5 2.0	2.5 2.5
CD0588X	7/22/99			80	2.0	2.5
		04055	8/1/96	80	2.0	2.5
		04056	8/1/96	20 20 20 80	0.05 0.5 5.0 2.0	0.25 2.5 25 2.5
		04162	8/1/96	20 20 20 80	0.05 0.5 5.0 2.0	0.25 2.5 25 2.5
		04165	12/19/96	20 20 80	0.5 5.0 2.0	2.5 25 2.5
		04233	12/19/96	20 20 80	0.5 5.0 2.0	2.5 25 2.5
		04240	12/19/96	80	2.0	2.5
		04244	12/19/96	20 20 20 80	0.05 0.5 5.0 2.0	0.25 2.5 25 2.5
		04245	12/19/96	20 20 20 80	0.05 0.5 5.0 2.0	0.25 2.5 25 2.5
		04250	12/19/96	80	2.0	2.5

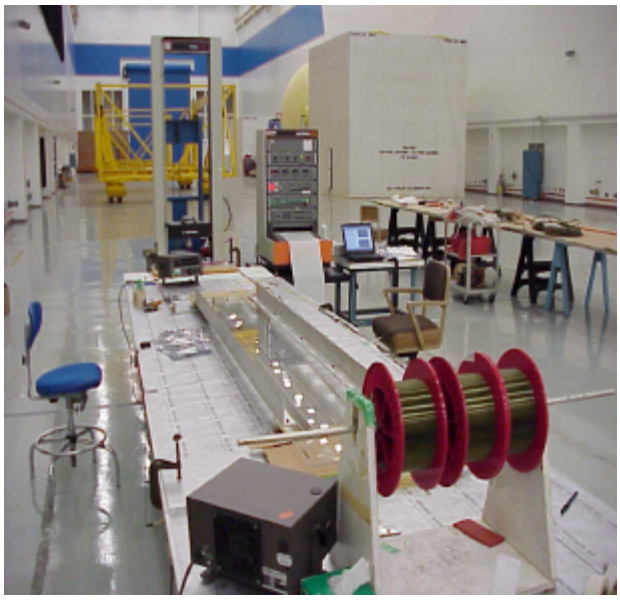

Courtesy of The Boeing Corporation

Figure 29 Test Set-up

7.1.2.1 Results: Initial Tests on Cabled Fiber

The results of the initial strength tests are shown in the Weibull plots in Figures 30 and 31. Prior analysis showed that the fiber shipped by Lucent-SFT was proof tested to 141 kpsi (@ 3.36 lbs). The cable specification requirement is for a fiber strength of 200 kpsi (@ 4.76 lbs). Lindholm, et. al., report strengths of 500 kpsi (11.90 lbs) and higher for four carbon coated fibers they have manufactured. The plots showed the high strength of the cabled fiber to be around 252 kpsi (6 lbs) and the low strength to go as low as 126 kpsi (3 lbs).

The inspections found that defects were present in large numbers that were either small etch pits at the surface of the cladding or corrosion sites in the same location. The knees in the Weibull plots, an associated slopes, show that there is more than one dominant failure mode. According to the physics of glass, the order of the curves should show the black circles (highest strain rate) located to the right of the other curves, not to the left. Figure 31 shows that the distribution of low strength breaks among the reels was significantly different even for reels with the same date of manufacture. These distributions could not be used to quantify the expected life of the cable using classical methods.

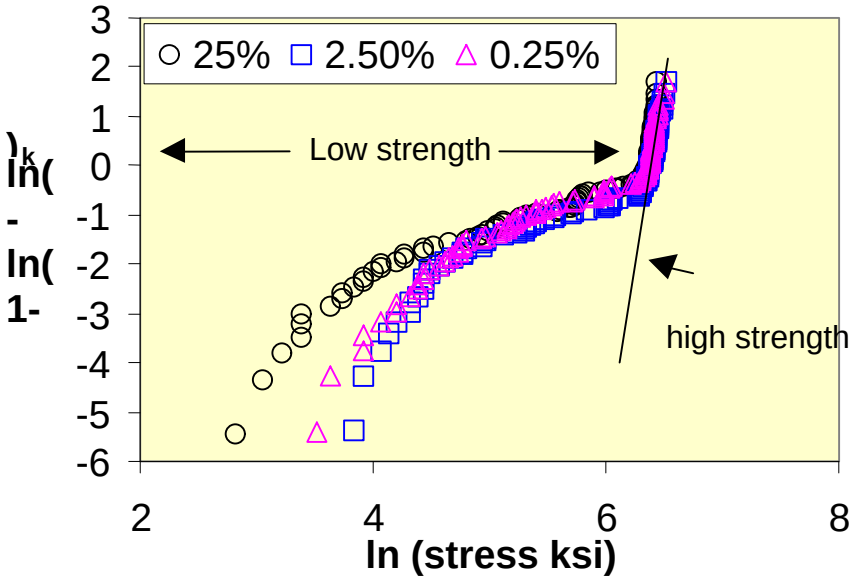

Figure 30 Weibull Plot for Strength of 1996 Vintage Cable from Several Cable Reels

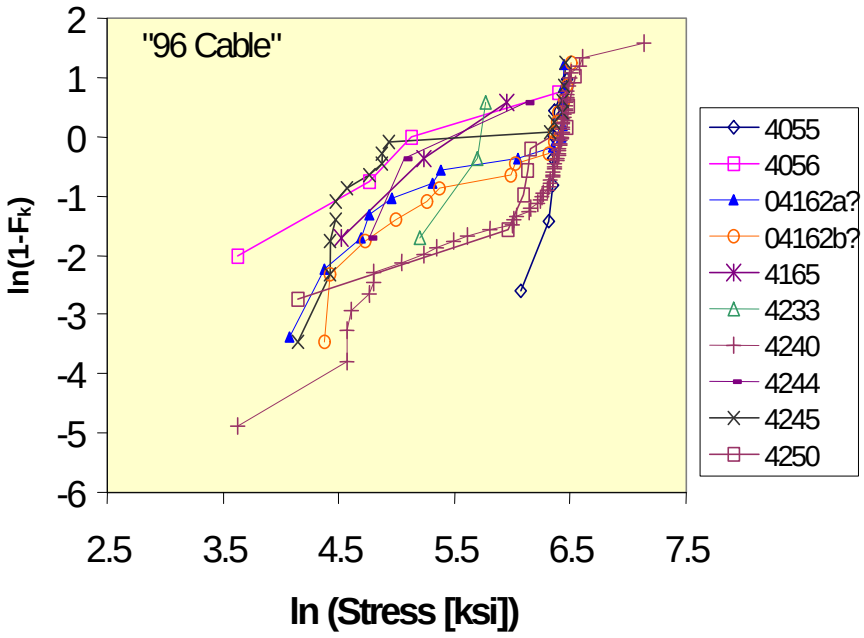

Figure 31 Strength Data for 1996 Cable by Strain Rate

7.2 Strength Testing of Fiber Throughout Cabling and Including HF Exposure

The results of the initial testing showed that more than one type of defect is affecting the strength of the cabled fiber. A second round of strength testing was performed to look at each of the cabling process steps' affect on the cabled fiber strength. The significant process steps studied were: respooling, buffering, strength member application and jacketing. After each of these steps, the fiber was strength tested and samples were exposed to HF vapor. Table 9 shows the test approach.

Table 9 Second Strength Test Approach

				Remaining Sample Lengths at End of Test/Operation (meters)					
Seq. #	**Operation or Test**	**Length Used**	**Test Location**	**CDO384XB (Control)**	**CDO384XC (HF)**	**CDO384XE (Strength)**	**CDO588XB (HF)**	**CDO588XC (Strength)**	**CDO588XD (Control)**
	Starting Sample Lengths	(m)		1870	489	483	518	809	935
1	Visible Fault Location			1870	489	483	518	809	935
2	Initial Dynamic Tensile Strength Tests			1847	460	459	504	787	918
3	OTDR (850nm??)		BHB	1847	460	459	504	787	918
4	Loss (1300nm)		BHB	1847	460	459	504	787	918
5	Retain Individual Control Sample	50	BHB		410	409	454	737	
6	Remove HF Etch Samples	10	BHB		400		444		
7	Remove Dynamic Tensile Samples	30	BHB			379		707	
8	Dynamic Tensile Strength		BHB						
9	HF Exposure/Visual Exam		GSFC						
10	Respool/Laser Mike Exam		BICC		400	379	444	707	
11	Visible Fault Location		BICC		400	379	444	707	
12	Remove Dynamic Tensile Samples	30	BICC			349		677	
13	Remove HF Etch Samples	10	BICC		390		434		
14	Dynamic Tensile Strength		BHB						
15	HF Exposure/Visual Exam		GSFC						
16	Extrude FEP Loose Tube Buffer	40	BICC		350	309	394	637	
17	Visible Fault Location (respool?)		BICC		350	309	394	637	
18	Remove Dynamic Tensile Samples	30	BICC			279		607	
19	Remove HF Etch Samples	10	BICC		340		384		
20	Dynamic Tensile Strength		BHB						
21	HF Exposure/Visual Exam		GSFC						
22	Apply Strength Member		BICC		340	279	384	607	

Table 9 Second Strength Test Approach (Cont'd)

				Remaining Sample Lengths at End of Test/Operation (meters)					
Seq. #	**Operation or Test**	**Length Used**	**Test Location**	**CDO384XB (Control)**	**CDO384XC (HF)**	**CDO384XE (Strength)**	**CDO588XB (HF)**	**CDO588XC (Strength)**	**CDO588XD (Control)**
23	Visible Fault Location (respool?)		BICC		340	279	384	607	
26	Dynamic Tensile Strength		BHB						
29	Visible Fault Location (respool?)		BICC		290	209	334	537	
30	Remove Dynamic Tensile Samples	30	BICC			179		507	
31	Remove HF Etch Samples	10	BICC		280		324		
32	Dynamic Tensile Strength		BHB						
33	HF Exposure/Visual Exam		GSFC						

[ref-21]

7.2.1 Results: Strength Testing of Fiber Throughout Cabling and Including HF Exposure

The results of the second round of strength testing are shown in Figures 32a through 32d. [ref-22, 23, 24] Figures 33a through 33d show the endfaces of the fibers at the low strength breaks.

a.

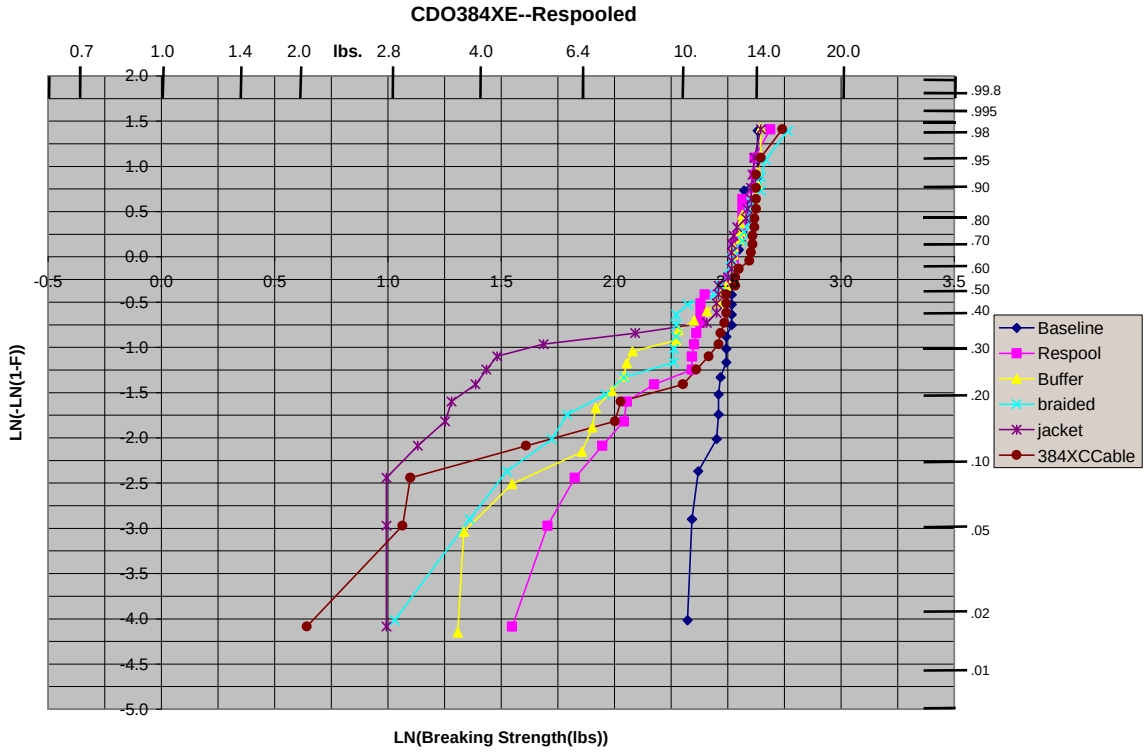

b.

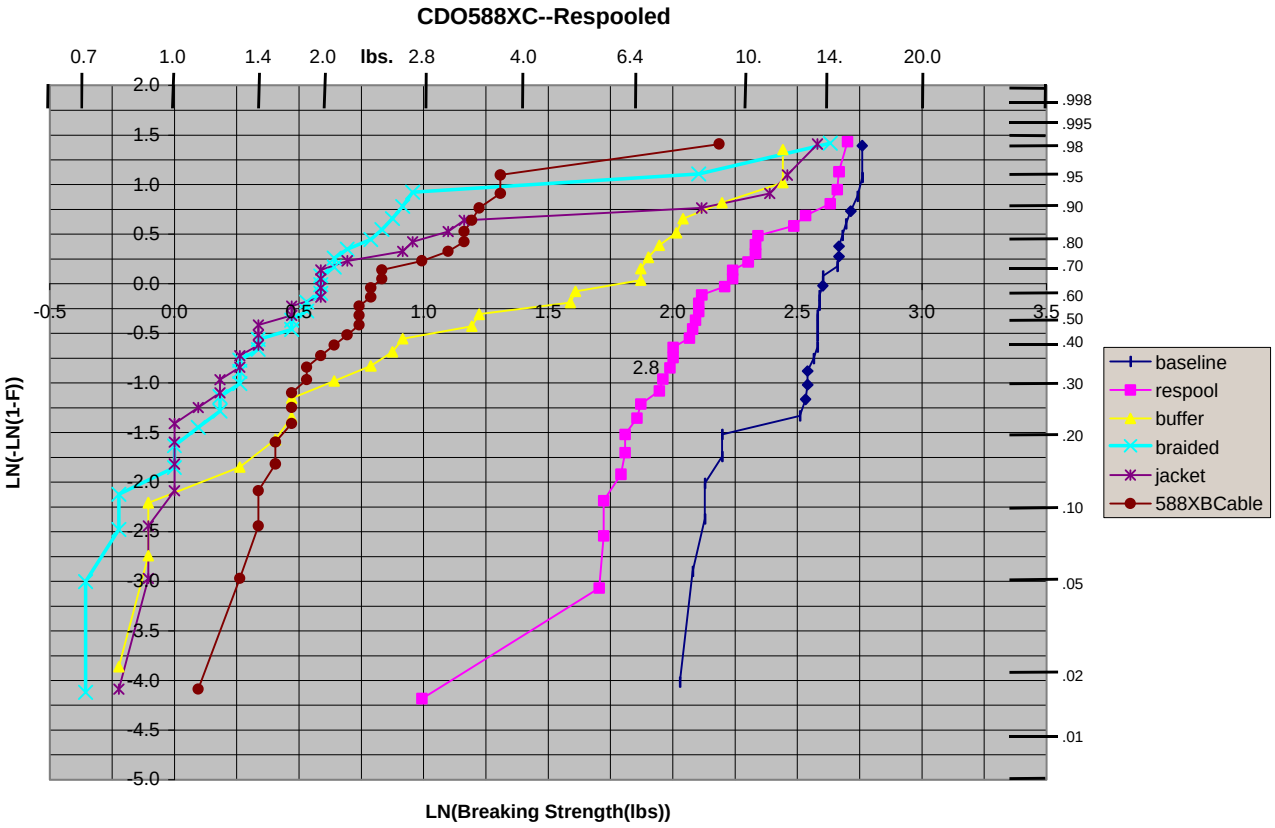
CDO588XC--Respooled
0.7
1.0
1.4
2.0
lbs.
2.8
4.0
6.4
10.
14.
20.0
2.0
1.5
1.0
0.5
0.0
-0.5
-1.0
-1.5
-2.0
-2.5
-3.0
-3.5
-4.0
-4.5
-5.0
-0.5
0.0
0.5
1.0
1.5
2.0
2.5
3.0
3.5
2.8
.998
.995
.98
.95
.90
.80
.70
.60
.50
.40
.30
.20
.10
.05
.02
.01
LN(-LN(1-F))
LN(Breaking Strength(lbs))
baseline
respool
buffer
braided
jacket
588XBCable

c.

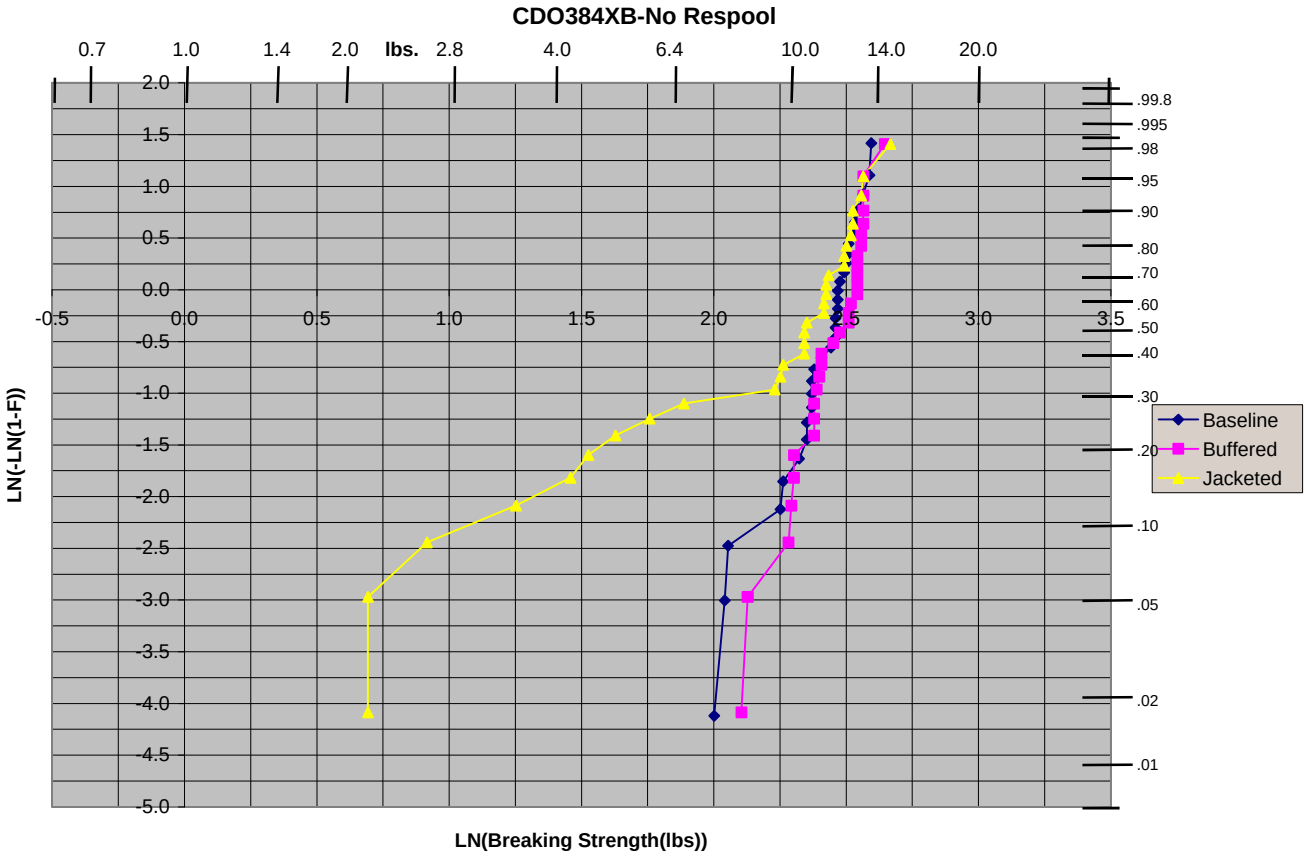
CDO384XB-No Respool
0.7
1.0
1.4
2.0
lbs.
2.8
4.0
6.4
10.0
14.0
20.0
2.0
1.5
1.0
0.5
0.0
-0.5
-1.0
-1.5
-2.0
-2.5
-3.0
-3.5
-4.0
-4.5
-5.0
-0.5
0.0
0.5
1.0
1.5
2.0
2.5
3.0
3.5
.99.8
.995
.98
.95
.90
.80
.70
.60
.50
.40
.30
.20
.10
.05
.02
.01
LN(-LN(1-F))
LN(Breaking Strength(lbs))
Baseline
Buffered
Jacketed

d.

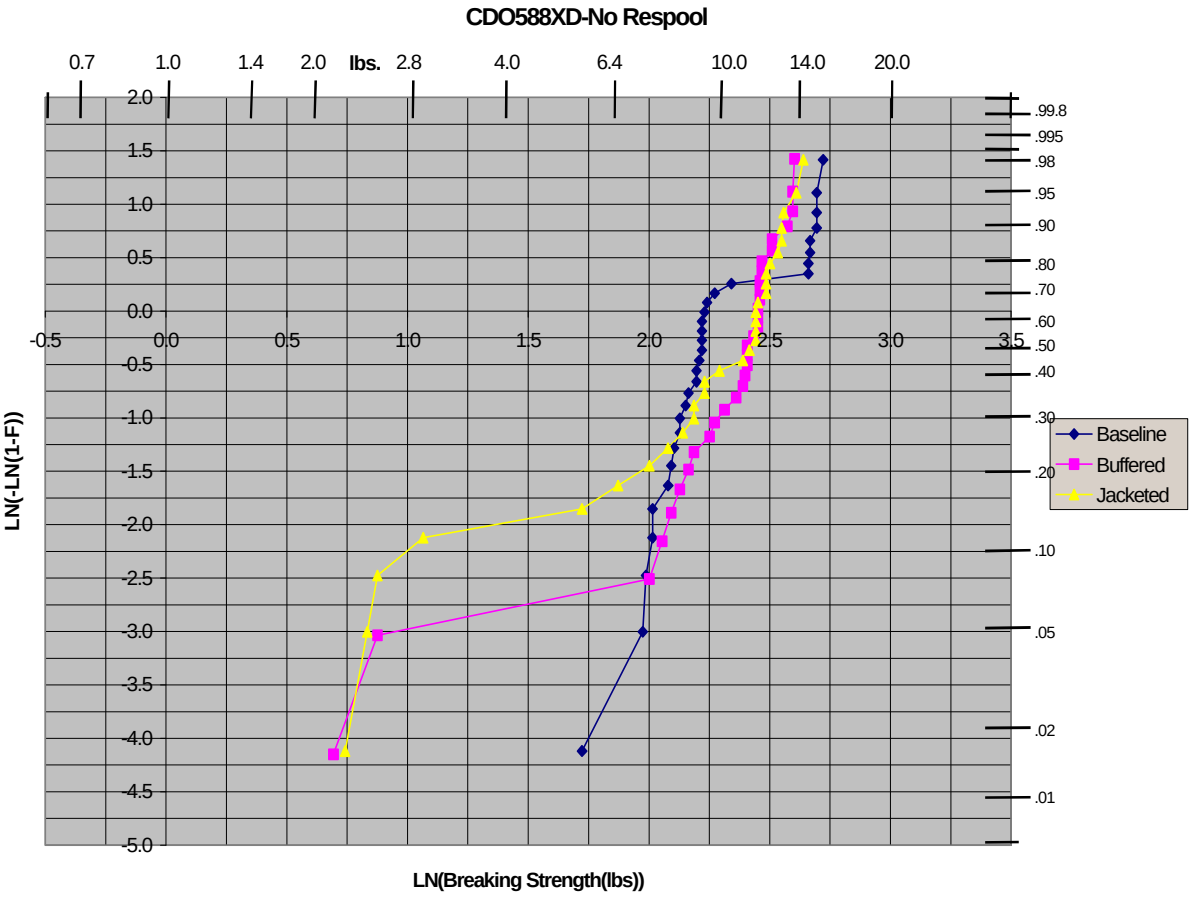

Figure 32 Strengths of DC0384 and DC0588 Fiber During Cabling

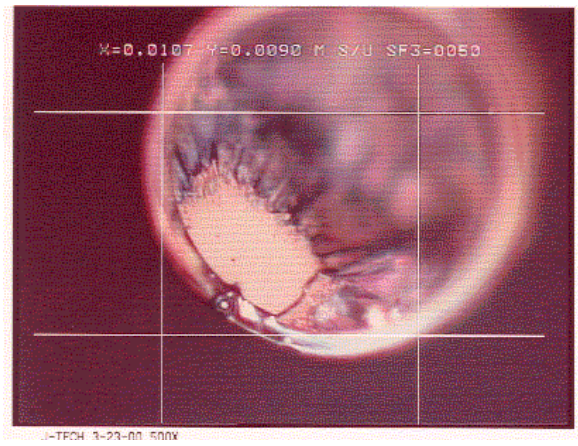

a. Stationary Fixture End, Fiber CD0588XCB, CD0588XCB, Sample 11

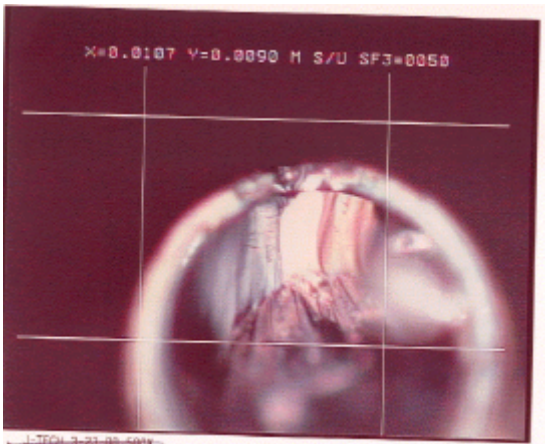

b. Moving Fixture End, Fiber Sample 11

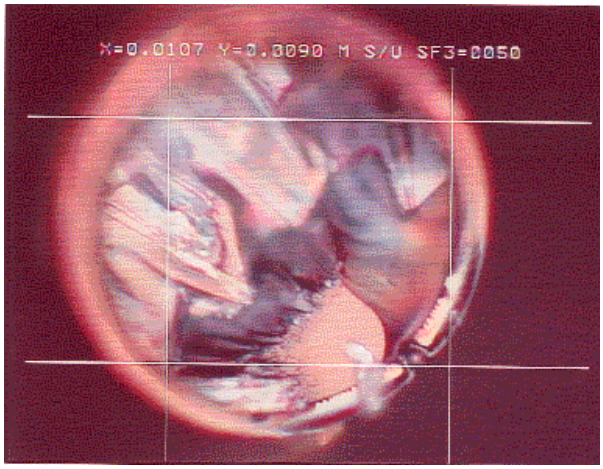

c. Stationary Fixture End, CD0588XCB, Buffered, Sample 11

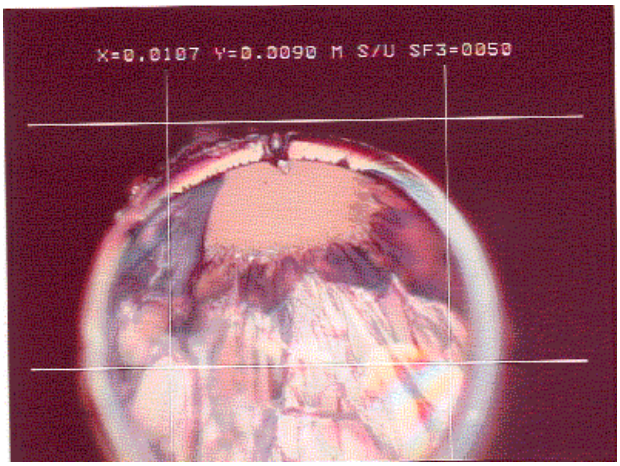

d. Moving Fixture End, Fiber, CD0588XCB, Buffered, Sample 11

Figure 33 Example of Low Strength Breaks

Figure 32a through 32d show that the fiber starts the process with high strength and every process step seems to weaken it, including the respooling process. They also show that the 588 fiber lot experienced greater weakening due to the cabling process that the 384 lot did, though they started with similar baseline strength. More bubbles were found in the polyimide coating during DPA on the 588 samples than on the 384 samples leading to continued interest in the correlation between the presence of the bubbles and latent defect sites.

Exposure to HF was used to try to measure the increase in etch related defects due to the respool and buffering cabling processes. Table 10 shows the results of this testing. The results point again to the propensity of the 588 lot to allow etch related defects versus the 384 lot. The 384 lot in this test, appears to be more robust with respect to defect creation or exacerbation associated with the respooling process. Figures 34a and 34b show the optical throughput during the etching period. [ref-25]

Table 10 HF Etch Results

Run #	Sample ID	Condition	Monitor wavelength	Total time	Time to change	#Breaks	#Scatters
			(nm)	hr:min	min		
1	CDO588XBRS#1	after respool	632.8	0:48	0:44	7	14
2	CDO588XBRS#2	after respool	632.8	2:10	1:06	3	16
3	CDO384XCRS#1	after respool	632.8	2:53	0:35 to 0:39	0	2
4	CDO384XCRS#2	after respool	1310	2:55	NA	0	1
5	CDO384XCCP#1	before respool	1310	1:17	0:17	1	0
6	CDO384XCCP#2	before respool	1310	2:33	NA	0	0
7	CDO588XBCP#1	before respool	1310	2:02	NA	1	0
8	CDO588XBBF#1	after buffer, in tube	1310	2:40	NA	0	0
9	CDO588XBBF#2	after buffer, removed from tube	1310	1:29	0:45	3	34
10	CDO384XCBF#1	after buffer, removed from tube	1310	2:22	1st 0:11	0	2
					2nd 1:30		

In all cases approximately 8 meters of fiber was subjected to HF vapor; approximately 1.5 to 2 meters was required to attach to monitoring equipment

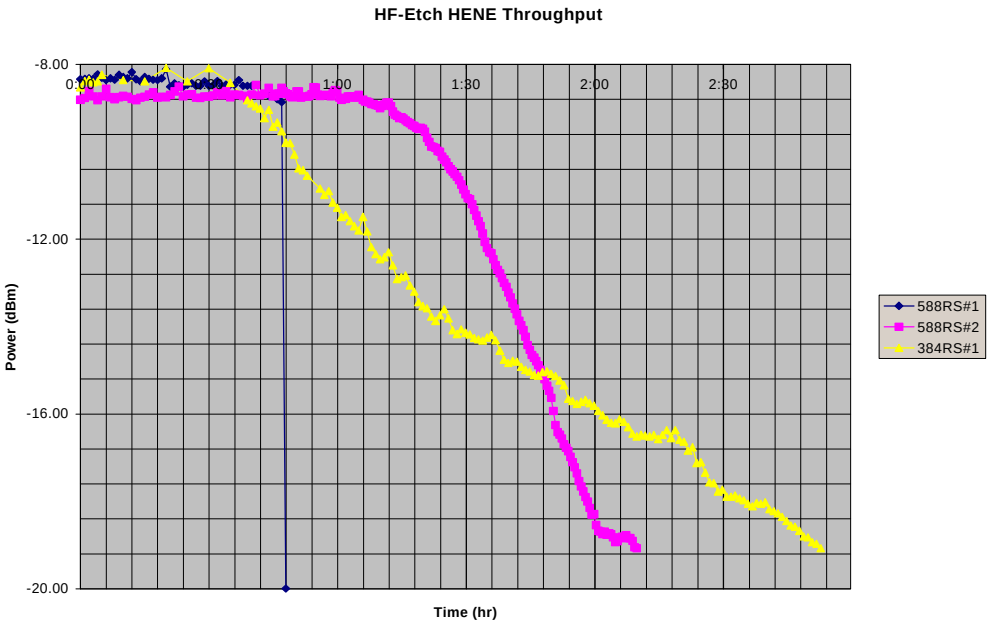

a. Run 1 through 3 with a HeNe source

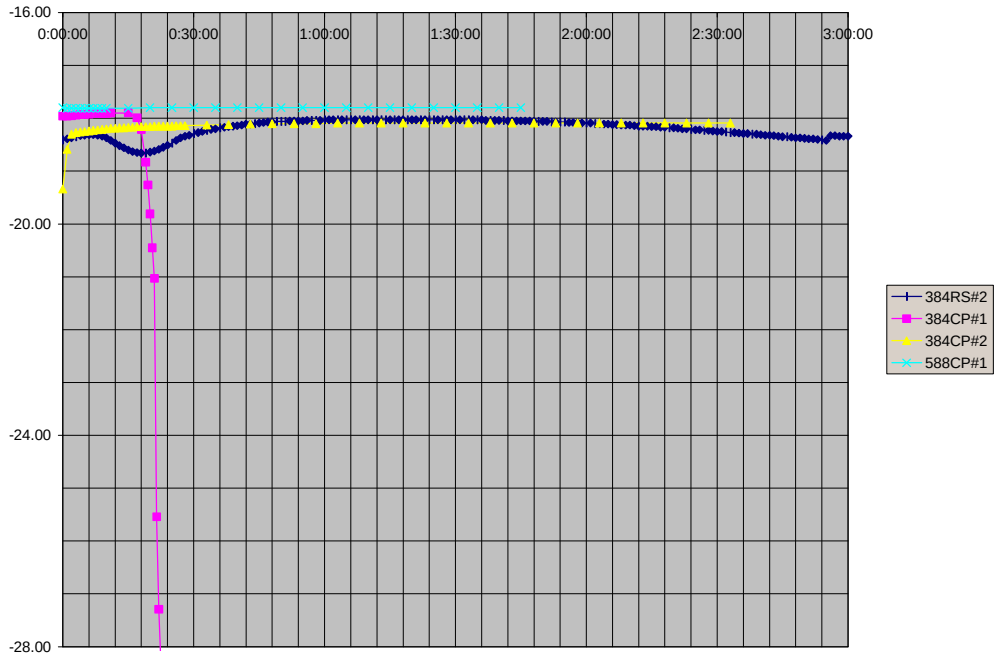

b. Run 4 through 7 with an 1030 LED source

Figure 34 Optical Throughput During HF Etch Test

7.3 Strength Testing Non-Carbon Coated Fiber

A third round of testing was performed to see if the weakening of the fiber due to the respooling process was unique to the carbon coated fiber. Table 11 shows the test plan used.

Table 11 Test Plan for Strength Testing of Non-Carbon Coated Fiber

Sequence #	Operation or Test	Length used (m)	Facility	CDO384XB	CDO588XD	CDO858XB1	CDO731XB
	Starting Sample Lengths			1847	918	2200	2200
1	OTDR/Visible Fault location	NA	BICC			2200	2200
2	Loss (1300 nm)	1	BICC			2199	2170
3	Retain Top of Spool Individual Control Sample	50	BICC			2149	2120
4	Baseline Dynamic Tensile Strength Samples	30	BICC			2119	2090
5	Baseline HF-Etch Samples	30	BICC			2089	2060
6	Retain Top of Spool Individual Control Sample	50	BHB	1797	868		
7	Baseline Dynamic Tensile Strength Samples	30	BHB	1767	838		
8	Baseline HF-Etch Samples	30	BHB	1737	808		
9	Respool/LaserMike™/Current & Field Probe	150	BICC	1587	658		
10	Respool/LaserMike™/Current & Field Probe	600	BICC			1489	1460
11	OTDR/Visible Fault location	0	BICC			1489	1460
12	Remove Dynamic Tensile Strength samples	30	BICC				
13	Remove HF-etch samples	30	BICC				
14	Extrude loose tube buffer	540	BICC	1047	118	949	920
15	Retain End of Section Individual Control Sample	50	BICC	997	68	899	870
16	Remove EOS Dynamic Tensile Strength Samples	30	BICC	967	38	869	840
17	Remove End of Section HF-Etch Samples	30	BICC	937	8	839	810
18	Remove excess fiber from process account			0	0	0	0
19	Extrude loose tube buffer	40	BICC				
20	Insert Buffered fibers (step 14) into remaining steps			500	500	500	500
21	OTDR/Visible Fault location	0	BICC	500	500	500	500
22	Remove Dynamic Tensile Strength samples	30	BICC	470	470	470	470
23	Remove HF-etch samples	30	BICC	440	440	440	440
24	Apply strength member	0	BICC	440	440	440	440
25	OTDR/Visible Fault location	0	BICC	440	440	440	440
26	Remove Dynamic Tensile Strength samples	30	BICC	410	410	410	410
27	Remove HF-etch samples	30	BICC	380	380	380	380
28	Extrude Jacket	40	BICC	340	340	340	340
29	OTDR/Visible Fault location	0	BICC	340	340	340	340
30	Remove Dynamic Tensile Strength samples	30	BICC	310	310	310	310
31	Remove HF-etch samples	30	BICC	280	280	280	280
32	Complete Dynamic Strength Tests-Baseline Samples		BHB				
33	Complete HF-Etch Tests-Baseline Samples		BHB				
34	Complete Dynamic Strength Tests-Respool Samples		BHB				
35	Complete HF-Etch Tests-Respool Samples		BHB				

Table 11 Test Plan for Strength Testing of Non-Carbon Coated Fiber *(Cont'd)*

Sequence #	Operation or Test	Length used (m)	Facility	CDO384XB	CDO588XD	CDO858XB1	CDO731XB
36	Complete Dynamic Strength Tests-Braided Samples		BHB				
38	Complete Dynamic Strength Tests-Jacketed Samples		BHB				
39	Complete HF-Etch Tests-Jacketed Samples		BHB				
40	Complete Dynamic Strength Tests-EOS Samples		BHB				
41	Complete HF-Etch Tests-End of Section Samples		BHB				
	Virgin Fiber Left at end of tests			937	8	839	810

The fiber from the non-carbon coated lots, CD0858XB1 and CD0731XB are polyimide coated but do not have the carbon under-layer. The Lucent-SFT product number for this fiber is BF04455. The preform is SG320, not the rad-tolerant "320R" type used in the preform used to make BF04515 fiber.

7.3.1 Results: Strength Testing Non-Carbon Coated Fiber

Figure 35a through 35c show the affect of the various cabling processes on the fiber strength for the non-carbon-coated fibers. The unprocessed fiber has high strength, however as it goes through cabling, its strength is again increasingly reduced. The difference in the behavior between the two non-carbon coated fiber lots is still under study. [ref-26]

a.

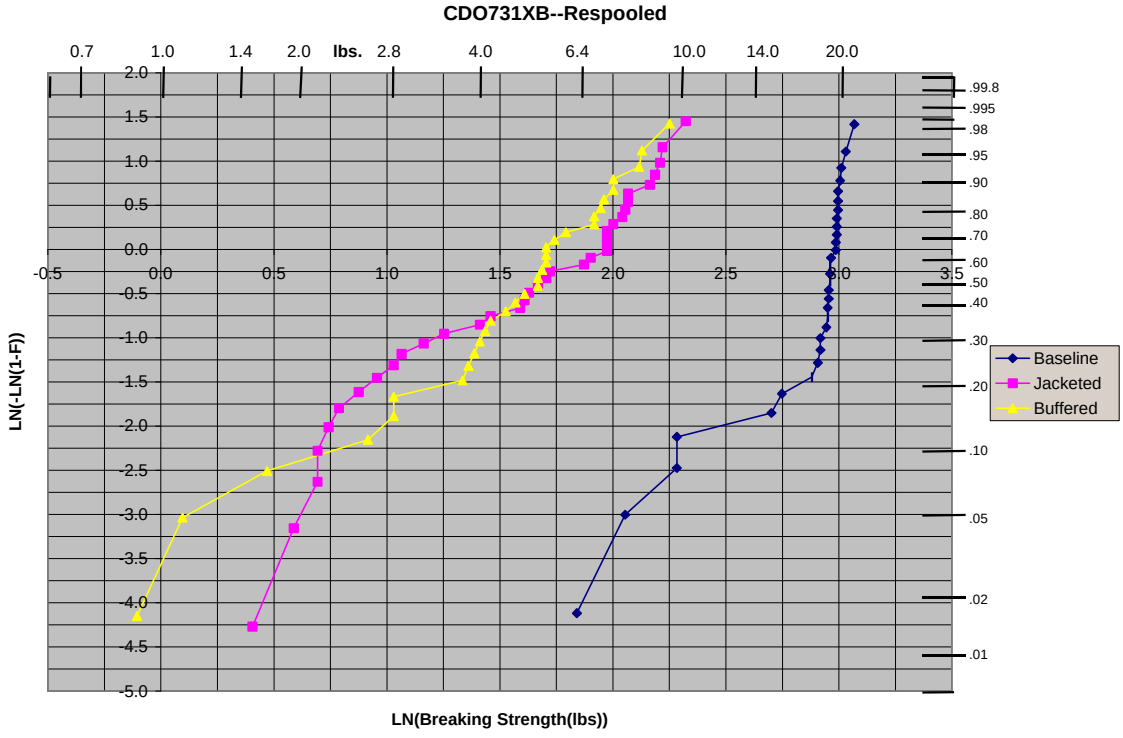

b.

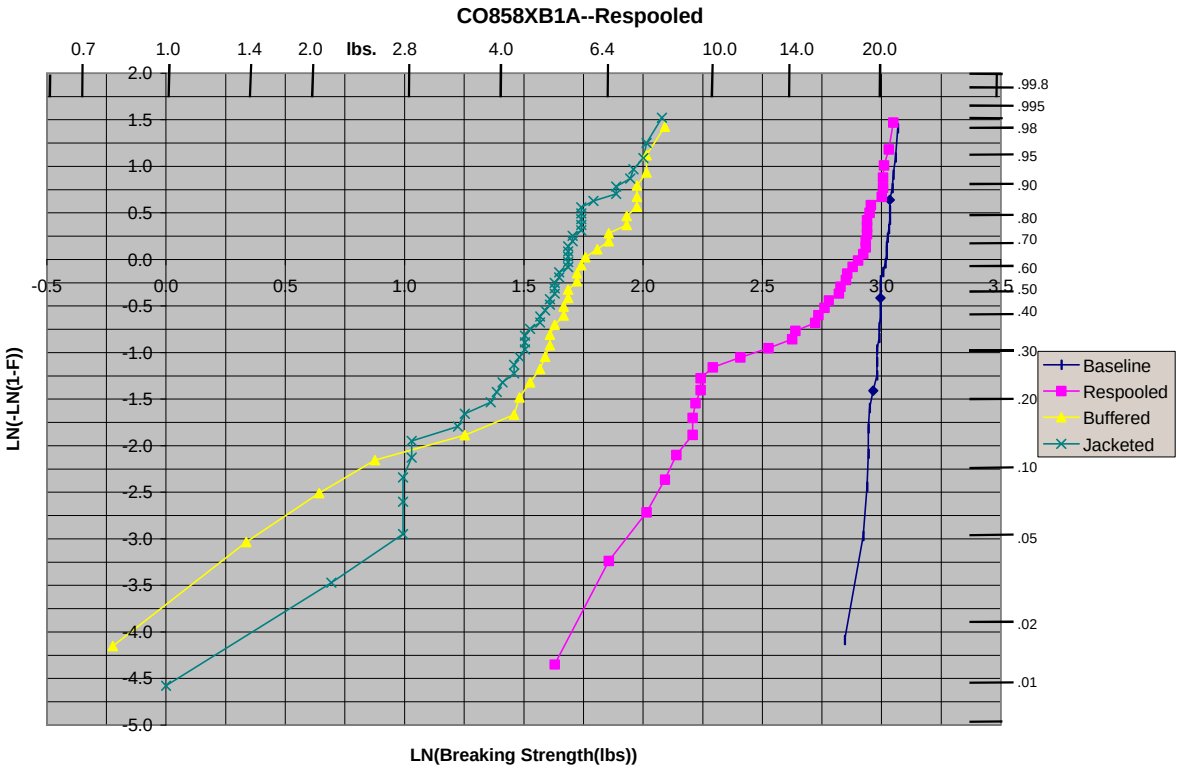
CO858XB1A--Respooled
0.7
1.0
1.4
2.0
lbs.
2.8
4.0
6.4
10.0
14.0
20.0
2.0
1.5
1.0
0.5
0.0
-0.5
-1.0
-1.5
-2.0
-2.5
-3.0
-3.5
-4.0
-4.5
-5.0
-0.5
0.0
0.5
1.0
1.5
2.0
2.5
3.0
3.5
.99.8
.995
.98
.95
.90
.80
.70
.60
.50
.40
.30
.20
.10
.05
.02
.01
LN(-LN(1-F))
LN(Breaking Strength(lbs))
Baseline
Respooled
Buffered
Jacketed

c.

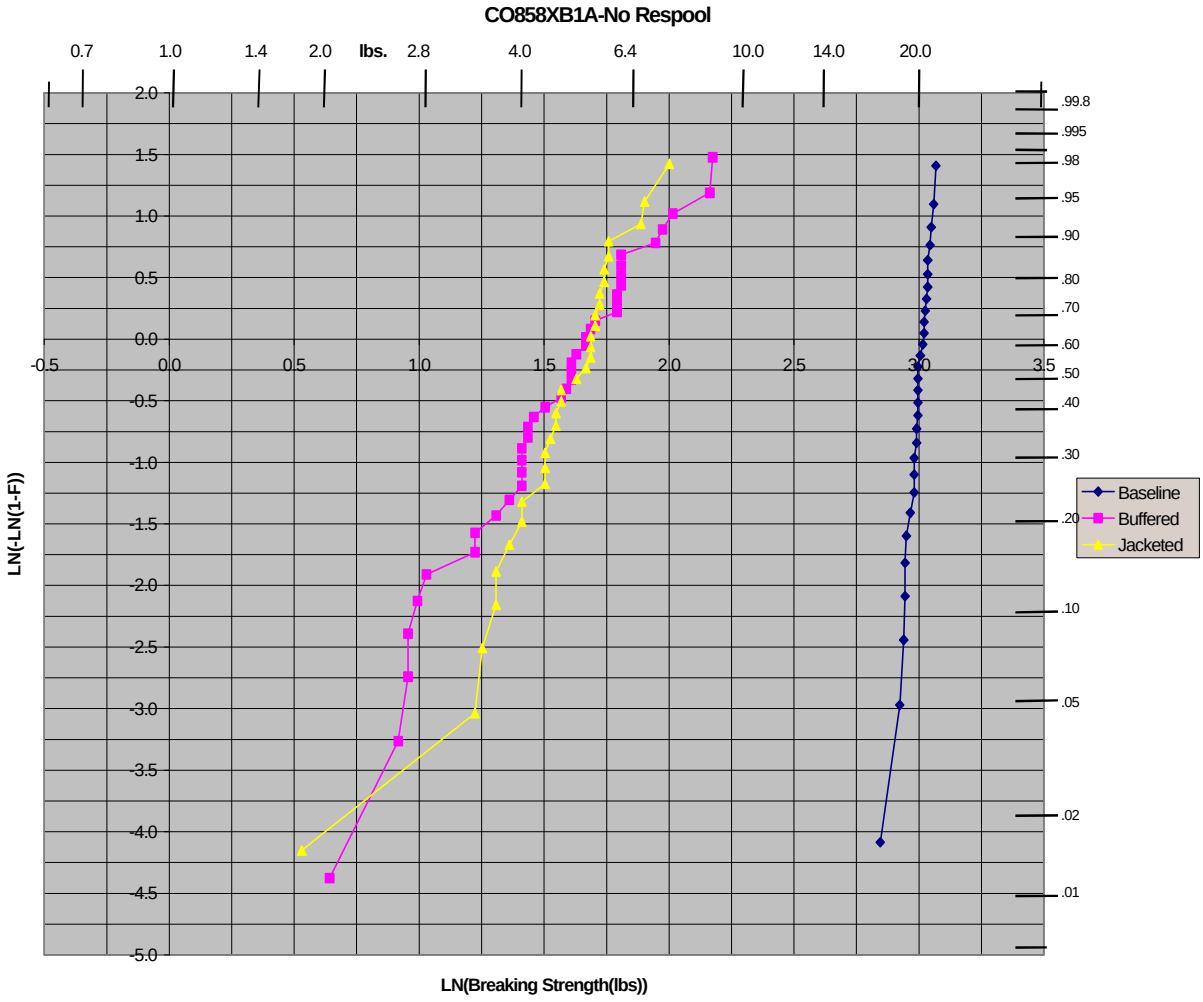

Figures 35 Strength for the Non-carbon Coated Fibers

7.4 Mandrel Test Screening of Cabled Fiber

Testing was performed to determine if a mandrel proof test could be performed as an incoming screen to remove low strength fiber. Figure 36a and 36b shows the mandrel arrangements and sizes used. Lengths from cable lot 04245 and 04255 had been strength tested as discussed in section 7.1 above. The 04245 lot was found to contain more low strength sites than 04250 though the 04250 lot also had similarly weak links. Both of the samples were screened for glows with a HeNe laser and for echoes with an OTDR. This established that the 04245 sample was starting the evaluation with at least one flaw. No glows were found for the 04250 sample and no echoes were found for either. The samples were then submitted to the proof test, which extended roughly 100 kpsi (2.4 lbs) to the cable.

The fracture surfaces of the breaks found in the 04250 sample were analyzed and breaking strengths in lbs were calculated for them. These have been superimposed on the curve of breaking strengths found for the surviving sample, which was strength tested after the mandrel wrap screen. The lower (blue) section of Figure 37 represents the calculated values. The blue portion of the curve in Figure 38 are extrapolated values for the breaks, which occurred during the mandrel wrap screen in the 04245 sample. Figure 39 shows the dynamic strength data alone.

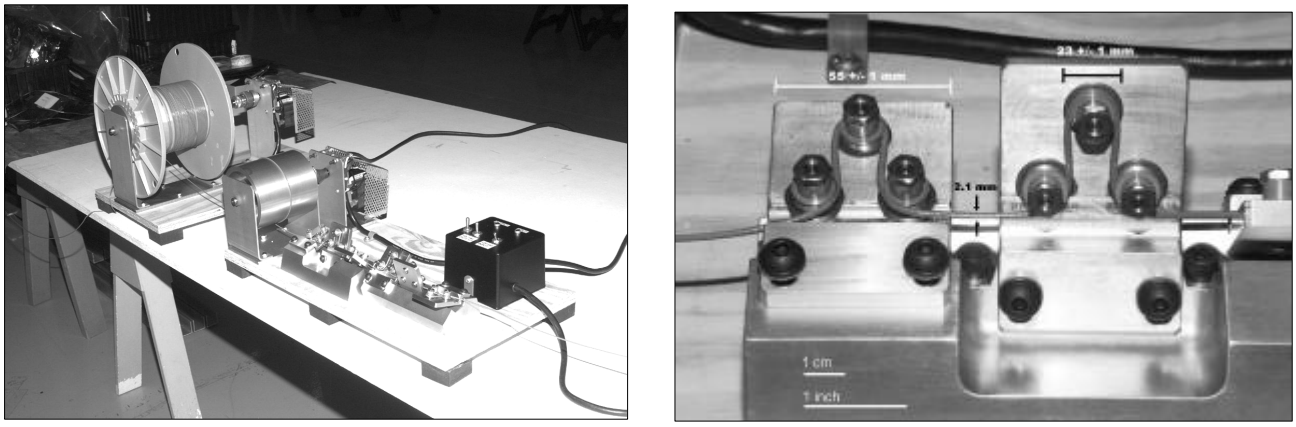

a. *b.*

Figure 36 Mandrel arrangements and Sizes Used

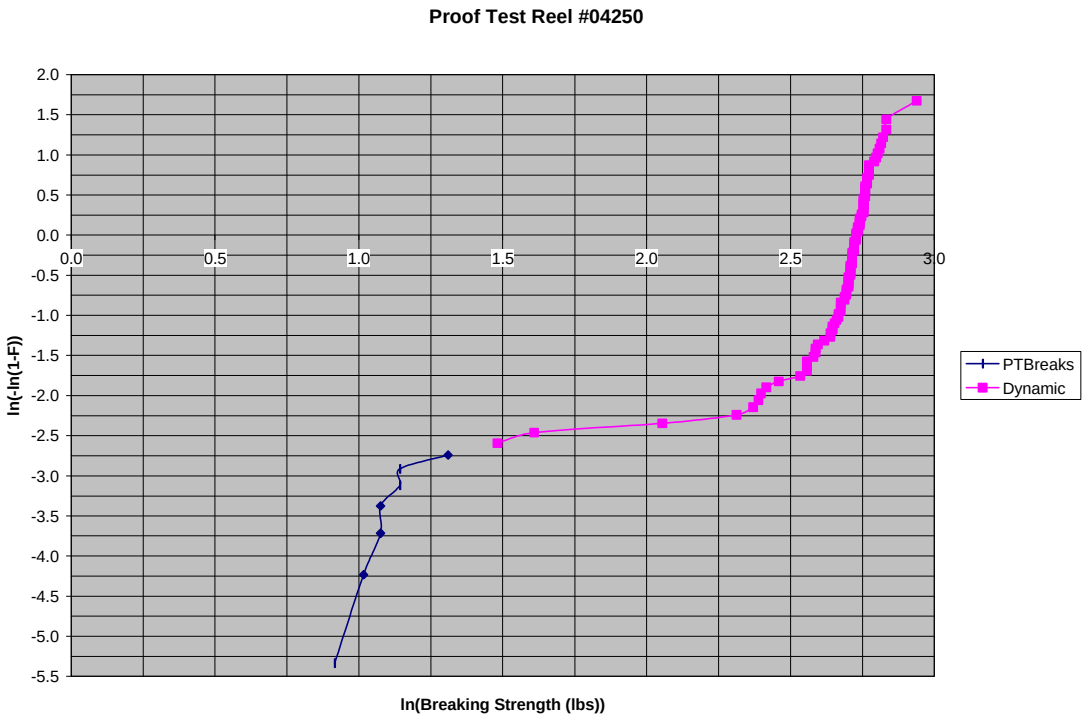

Figure 37 Hypothetical Break Strengths During Screen Compared to Actual Break Strengths on Proof Test Screened Sample

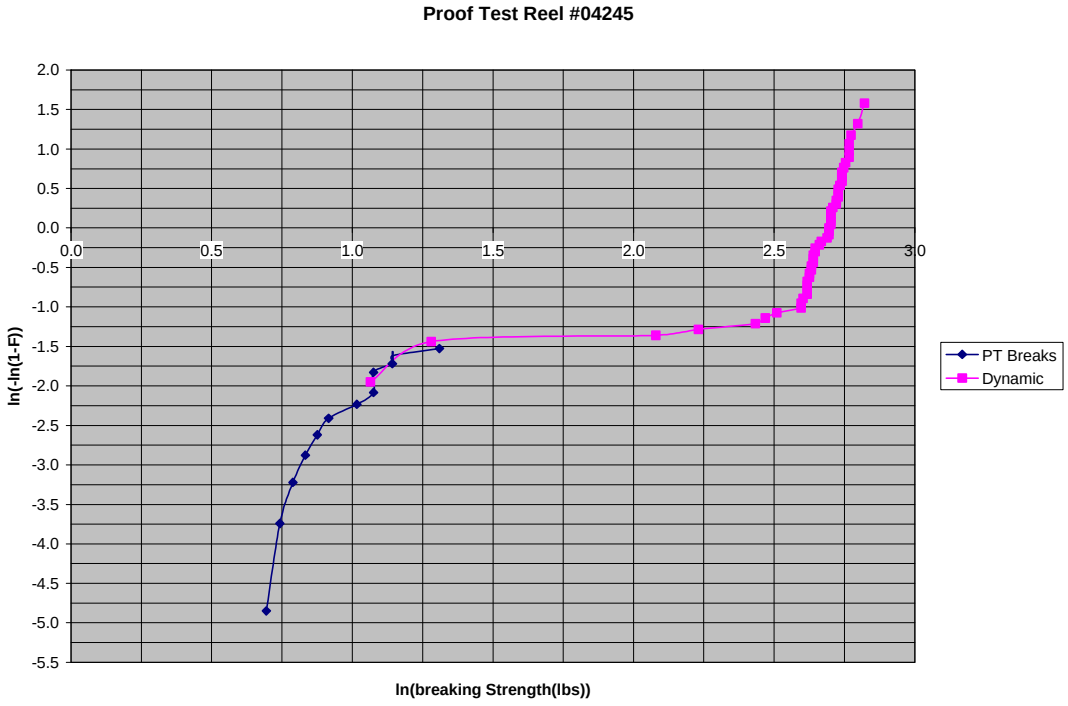

Figure 38 Mandrel Used for Screening Evaluation

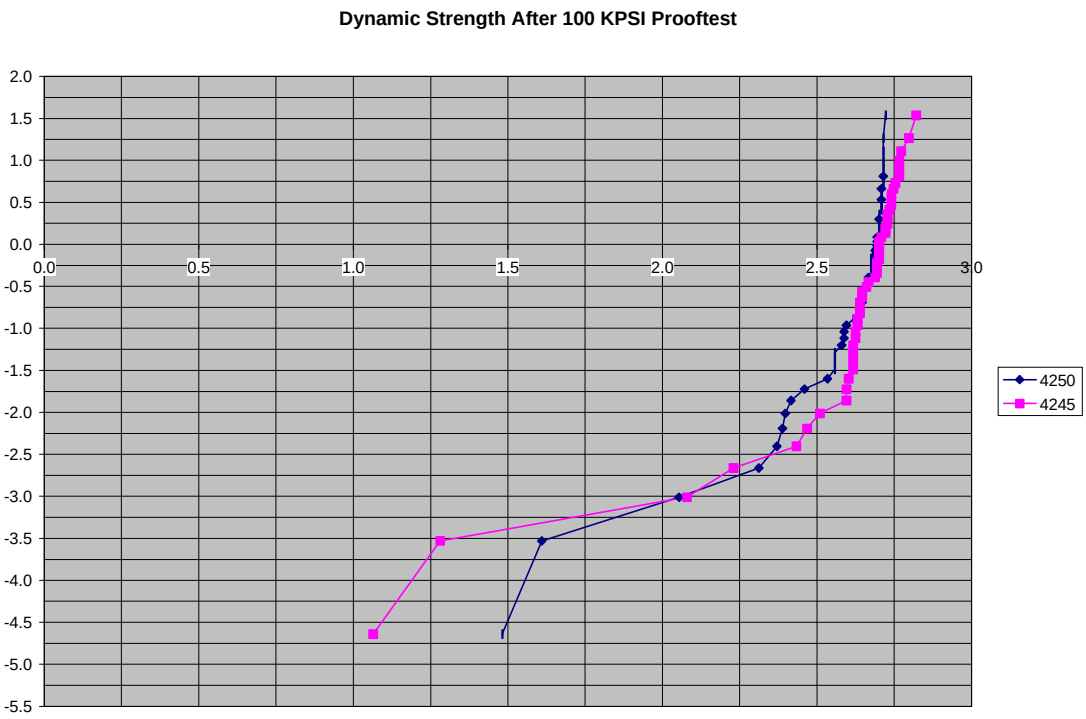

Figure 39 Dynamic Strength Data for the Pre-Proof Test Screened Cables

8.0 CONCLUSIONS

The cable design which has been associated with “rocket engine” defects, within the optical fiber, and later with low breaking strengths of the fiber, has been that defined by the ISS specification SSQ21654 (plus engineering modifications) and given the Boeing Company part number NFOC-2FFF-1GRP-1. Some small amounts of a similar part number, NFOC-2TFF-1GRP-1 was also used in ISS hardware; however, the problem investigation reported here does not concern this second part number. The production period of concern spans between June of 1996 to July of 1999. End users were Boeing-HB, ISS partners, and their subcontractors.

The fiber and cable build history indicates only two major process changes over the period in which the NFOC-2FFF-1GRP-1 was made; (1) use of different draw towers at different plants of the fiber manufacturer, and (2) implementation of a respooling operation at the cabling plant. Upon initial review, the available traceability data did not conclusively indicate that these process changes were the sole cause of the “rocket engine” defect. The investigation has brought into light a better understanding of the latency of the defects, warranting another review of the traceability data for pointers to weaker cable lots.

The manufacturing process review identified several processes that contribute to the creation of “rocket engine” defects and of fiber strength reducing defects. Though none of the processes used are outside of normal practice for making specialty fiber or cable, they become uniquely undesirable for this cable because of the materials involved in this cable design.

The conditions present in the cabling processes, specifically with respect to the behavior of FEP at the temperature at which it is extruded while surrounded by air, create carbonal difluoride (COF_2). Carbonal Difluoride reacts with water resident in the polyimide to create hydrogen fluoride (HF) which etches the glass fiber wherever it is not covered by the carbon coating. The “rocket engine” defect is the result of HF etching, the products of which can be found in and around the etch pit and which are silica balls and germania crystals.

The root cause for the breaches in the carbon coating is still not understood well enough to predict the frequency of their occurrence. These breaches have been found to be 1 to 3 μm in size, and are often in the vicinity or directly below a distinct feature in the polyimide coating. This size makes them invisible to a screen, which uses electrical resistance as a measure of coating quality. The size may also make hydrogen ingression, and proof testing, incapable of identifying fiber that contains breaches at the rate of one per millimeter, or less. No practical screening method has been found which can be used to find these carbon breaches.

The polyimide features which accompany the “rocket engine” defects and low strength breaks have been found in at least three configurations: cups, buried voids (bubbles) and thinned areas (sink holes). Surface blisters are not being considered in this investigation. Data book values cannot be used to predict how the polyimide will perform mechanically and electrically because the polyimide is applied to the fiber in a way that differs substantially from the convention preparation of polyimide. Testing showed that the polyimide will break down at voltages between 3.5 kV and 4.0 kV where the features are not present, and at as little as 1.5 kV where thinning exists because of the presence of a feature. We believe that ESD events will be focused at the polyimide features because they reduce the dielectric’s thickness from 15 μm to as little as several micrometers. Though geometric analyses of the static fields measured around the fiber during fiber and cable manufacturing (specifically around the proof test during fiber manufacture and during respooling during cable manufacture) have not been done, it is believed that the actual potentials at the fiber surface during those processes are sufficiently high to support discharge events through the polyimide coating at these features. Testing showed that high current discharges will damage the polyimide severely and the carbon as well. It is believed that lower current events, which may not result in observable damage to the polyimide, are causing breaches in the carbon coating and the glass below it.

The co-location of the polyimide features and the carbon breaches has been shown; however, the preference for etching at some carbon breaches and not at others has not been explained. Periodicity has been seen with respect to the distribution of the etch sites and with respect to the distribution of the polyimide features. A better understanding of this periodicity may point to the process sources of the polyimide features and the carbon breaches.

Many screening and analysis methods were used in the study of this problem; some were successful and some others were not. Optical performance methods such as the use of commercial optical fault finders (OFF; 1 mW power) and specialty fault finders (OFF using 20 mW to 30 mW) tended to be more easily and successfully applied than the various OTDR's that are available. The farther the etch pit reached into the core, the more effective the OFF and OTDR screen was. Optical power meters were similarly useful: these detect deep etch pits. All three were not useful as a screening method when a shallow crack occurred in the exposed glass at a carbon breach (which reduces the fiber's life), but no etch pit removing waveguide material was present, which would effect the light throughput. In-line laser micrometers were not able to detect the polyimide surface features that indicate a fiber which contains latent defects. An IR laser based system may be useful in this way; however, more investigation will be required. Mandrel wrap screening gave promising results in its ability to screen low strength breaks from cabled fiber.

SEM and optical microscopy were very useful in DPA analyses. The use of index matching fluid was very useful for optical microscope inspection. X-ray has limited applicability with respect to fiber surface features however it is useful for understanding the configuration of fiber breaks still inside of the cable.

Strength testing has demonstrated the initial high strength of the fiber, even with the presence of what are believed to be latent defects. Prior study of carbon coated glass has shown it to have high strength over a wide range of strain rates. The Weibull plots of the breaking strength data for the respooled, partially cabled, and cabled fiber (using processes defined for NFOC-2FFF-1GRP-1) show that those cabling operations and other ancillary processes, including handling, introduce a population of low strength breaks into the BFO4515 fiber. The fiber was found to break with a distribution tail normally associated with non-hermetic glass whose surface defects are growing into cracks with handling stress. Non-hermetic fiber was tested throughout the cabling process as well and similar results were found.

Conventional n-theory-based life predictions could not be made using the dynamic fatigue data collected because it did not follow the basic laws of that theory. It is believed that one reason is that multiple failure modes were occurring in the fiber that was tested. Fiber life predicting using n-theory is designed for fiber whose only failure mode is crack propagation due to strain rate. It may not be impossible to develop similar predictive theory for the NFOC-2FFF-1GRP-1 system; however, it was outside of the scope of this investigation to accomplish that task.

9.0 RECOMMENDATIONS

The initial goal of this investigation was to understand the cause of the "rocket engine" defects found in the fiber contained in the NFOC-2FFF-1GRP-1 optical cable being used by Boeing in International Space Station hardware. It was believed that if the root cause of the rocket engine defect could be found, the handling or the manufacturing processes (or both) could be engineered to eliminate the defect from future hardware. As the investigation progressed, these defects began to be understood as distinct and related to synergistic processes occurring during fiber and cable manufacturing. While interest continued in tracking down the root causes of what was now a collection of defects, additional approaches to the problem resolution were explored. They included using screening to eliminate the defects from the product used to build flight hardware, and risk assessment to understand what level of defects may be tolerable given the reliability requirements established for ISS and the installation conditions used.

9.1 Processes Which Create Defects

It has been established that the cabling process being used to make the NFOC-2FFF-1GRP-1 cable, using the BF04515 fiber, will create COF_2 and ultimately HF. Processing FEP under dry nitrogen (to remove oxygen), during FEP processing and eliminating the water in the polyimide coating during buffer extrusion, will reduce the volume of HF produced during cabling by several orders of magnitude.

Breaches in the carbon on the fiber allow HF etching and strength reduction of the glass fiber. Direct inspections have shown the frequency of the etch pits varies widely along a given fiber and also varies between different fiber runs. More study of the carbon layer through materials analysis could provide insight into why this is so.

The frequency of polyimide features is also variable with the fiber draw lot. Their connection with carbon breaches and exposure of the fiber to ESD events of a lower strength than that afforded by a continuous, uniformly thick layer, indicates that they too should be eliminated. More study in many areas, including materials analyses and electrical and mechanical environmental analyses, is required to understand how the bubbles are formed. The development of successful screening methods for both carbon defects and the polyimide features will greatly contribute to understanding when the defects are occurring, as well as supporting the removal of these defects.

9.2 Screening Methods

The transparency of the fiber and its polyimide coating, and the fiber's geometry (especially its cylindrical shape and aspect ratio which is on the order of 10^9 to 10^{10}) make it extremely challenging to inspect. Screens, which can detect polyimide features, now associated with carbon breaches, should be developed to eliminate known latent defects. A similar screen for carbon breaches would be critically useful.

Dynamic strength testing should be used as part of a qualification; also, this testing should be repeated on some schedule. Development of the madrel wrap test should continued through repeatability and validation testing so that it can be demonstrated to be a non-destructive, 100% screen. Standardization of the test method through the EIA/TIA is also recommended. Future specification documents should use these tests to qualify and screen flight lots.

Lessons were learned during the investigation about improvements that could be made to the procurement specifications. Several improvements can be made with respect to specific definitions for fiber and cable production lots. Traceability of all finished cable harnesses back to all raw material lots and the fiber lot should be required. The fiber should be qualified by the end user and the cable specification should require use of qualified fiber in its construction (reference MIL-PRF-27500 for cable, which requires the use of MIL-PRF-22759 wire). The fiber lot should be defined and traceable back to the preform. The fiber and cable specifications should contain: lot-based screening (non-destructive, 100% basis, "Group A"), lot-based inspections (non-destructive and destructive mechanical and environmental tests, sample basis, every lot, "Group B" tests) and periodic qualification tests (destructive and non-destructive mechanical and environment tests and reliability validation, schedule based on production schedule, "Group C" tests). Self-auditing by the user should be used to confirm that the traceability requirements are being met.

The new failure modes associated with the etch pits and low strength will need to be addressed in the new specification. As new screens become available, as recommended above, they should be added to the specification.

9.3 Reducing Risks Associated with NFOC-2FFF-1GRP-1 Cable

Logistical and budget pressures will force the use in flight hardware of product produced by the same processes which created the latent defects and failures discussed in this report. Measures can be taken to reduce some of the risks associated with this cable stock. It has been established that the cable has an ESD sensitivity. This report states that a threshold of 1.5 kV was measured although that value could be less depending on the thinness of the polyimide at a defect site. More work could be done to further quantify the ESD sensitivity of this cable and to establish handling and installation requirements, which will protect the cable from ESD damage. It is strongly recommended that cablers and manufacturers of carbon coated fiber measure the electrostatic conditions in their plants and make modifications to equipment and handling processes which can introduce discharge events involving the fiber.

Any stress reduction that can be obtained by modifications to the installation plans for future builds will extend the life of this cable. Opportunities may exist for reducing stress on the cables when in-flight repairs are made where vibration conditions don't have to be accounted for (open supports rather than tie-downs can be used).

Finally, in order to gain insight about the rate at which the links are expected to break in flight, a static fatigue test (hanging weights from lengths of fiber in an environment at fixed temperature and humidity) should be performed.

10.0 REFERENCES

[ref-1: email: 3/20/00, From: William Weisenberger, "U.S. Lab ROM for Bending of Fiber"]
[ref-2: email: From: Ray Prestridge, RE: Fiber Optice, Attachment: SSQ_21654RB.PDF]
[ref-3: email: Ray Prestridge, "Words for 'PFA in ISS Node 1' paragraph", 7/23/00]
[ref-4: email: Henning Leidecker, "Fwd: RE: Fwd[2]:latest pictures", 11/12/99]
[ref-5: email: Brad Cothran, Boeing-KSC, "RE: Acceptance limit for finished harnesses", 3/14/00]
[ref-6: email: Dale Zevotek, "RE: OTDR that you use", Attachment: OC-1614.tif, 2/24/00]
[ref-7: Reference Manual, Model OFM, Optical Fiber Monitor, Opto-Electronics Inc., 1996]
[ref-8: C.T. Mueller and J.G. Coffer, "Polyimide/Carbon Defects", The Aerospace Corporation, 6/21/00]
[ref 9: Teflon Mechanical Design Data, Du Pont Company, no date]
[ref 10: Guide to the Safe Handling of Fluoropolymer Resins, The Society of the Plastics Industry, Inc., 1998]
[ref 11: Thermal degradation of commercial fluoropolymers in air, Bertsil B. Baker, Jr., Daniel J. Kasprzak, Polymer Degradation and Stability 42, 1993]
[ref-12: http://hdmicrosystems.com/2produts/prodlist.html]
[ref 13: The Nature of Water Absorbed by Polymeric Electronic Packaging Materials, Brian Dickens, G.T. Davis, http://www.nist.gov/msel/div854/electapps/1995_projects/nature3.html]
[ref 14: Moisture Effects in Electronic Packaging Polymers, no author, http://www.nist.gov/msel/div854/electapps/1996_projects/moisture2.html]
[ref 15: C.T.Mueller, J.G. Coffer, and T. Giants, "ISS Fiber Status", The Aerospace Corporation, 3/9/00]
[ref-16: email: D. DiGiovanni , "Re: Fw: Anyone have Jay Lee's new email address?", Lucent-Bell Laboratories, 4/26/00]
[ref-17: Eric A. Lindholm, Jie Li, Adam S. Hokansson, and Jaroslaw Abromczyk, Spectran Specialty Optics Company, and Sara E. Arthur, David R. Tallant, Sandia National laboratories, "Low Speed Carbon Deposition Process for Hermetic Optical Fibers", "International Wire and Cable Symposium, 1999".]
[ref-18: email: Craig Mueller, "Charts showing Carbon Pinhole and Bubble Defect Shape", 07/05/00]
[ref-19: Mallock, Proceedings of the Royal Society, vol 9, page 262, 1907]
[ref-20: A.B. Wood, "A Textbook of Sound: being an account of the physics of vibrations with special reference to recent theoretical and technical developments", 1930]
[ref-21: email: Gary Bickel, "Detail Coating Penetration Test Plan and Schedule", 3/15/00, Attachment: CoatingTstPln.xls]

[ref-22: email: Gary Bickel, Boeing-HB, FiberB&A.xls>> <<CoatingTestData.xls>> <<Respool384.xls>>, 3/25/00><<Respool588.xls>>]
[ref-23: email: Gary Bickel, Coating Penetration Tests: Strength Test Results on CD0588XB, 4/4/00]
[ref-24: email: Gary Bickel, Coating Penetration Tests: Strength Test on CD0588XC, 4/4/00]
[ref-25: Gary Bickel, Strength and HF-Etch Tests, 4/7/00]
[ref-26: Gary Bickel, "Revised Non-carbon-coated test Results", 7/18/00]

11.0 ACKNOWLEDGEMENTS

The Team 2, Root Cause Investigation Team, gratefully acknowledges the contributions of the following individuals whose efforts made this work and this report possible:

Jerry Arnett, The Boeing Company
Marvin E. Banks Jr., Boeing M&P, Kennedy Space Center
Harold Battaglia, The Boeing Company
Dave Beverly, NASA GSFC
Dr. Gary Bickel, The Boeing Company
Dr. John Canham, Unisys Corporation
Anna Cantwell, SEA Wire and Cable
Brad Cothran, The Boeing Company
David Gill, The Boeing Company
John Kolasinski, NASA GSFC
Dr. Henning Leidecker, NASA GSFC
Jim Holt, US Army Aviation & Missile Command
Jie Li, Lucent Specialty Fiber Technologies
Eric Lindholm, Lucent Specialty Fiber Technologies
Billy-Jo Mitchell, BICCGeneral
Carmen Moore, The Boeing Company
Pete Mueggler, The Boeing Company
Dr. Craig Mueller, The Aerospace Corporation
Mike O'Conner, Lucent Specialty Fiber Technologies
Melanie Ott, Sigma Research
Chris Pegge, BICCGeneral
Jeannette Plante, Swales Aerospace
Ray Prestridge, Lockheed-Martin Corporation
Dave Rothermel, BICCGeneral
Martin Seifert, Lucent Specialty Fiber Technologies
John White, The Boeing Company
Dale Zevotek, BICCGeneral

Special Thanks are extended for report production assistance to:

Jesse Frank, Swales Aerospace
Silvia Romero, Swales Aerospace
Carl Szabo, Swales Aerspace

Special thanks are extended for ISS Fiber website maintenance to:

Jesse Frank, Swales Aerospace